A COMPARISON OF SENTINEL 1 AND SENTINEL 2 IMAGE CLASSIFICATION FOR DETECTION OF WATER BODIES IN TURKIYE AND WORLD-WIDE

A THESIS SUBMITTED TO
THE GRADUATE SCHOOL OF NATURAL AND APPLIED SCIENCES
OF
MIDDLE EAST TECHNICAL UNIVERSITY

BY

BEN FORSYTH

IN PARTIAL FULFILLMENT OF THE REQUIREMENTS
FOR
THE DEGREE OF MASTER OF SCIENCE
IN
GEODETIC AND GEOGRAPHIC INFORMATION TECHNOLOGIES

SEPTEMBER 2024

Approval of the thesis:

A COMPARISON OF SENTINEL 1 AND SENTINEL 2 IMAGE CLASSIFICATION FOR DETECTION OF WATER BODIES IN TURKIYE AND WORLD-WIDE

Submitted by **BEN FORSYTH** in partial fulfillment of the requirements for the degree of **Master of Science in Geodetic and Geographic Informatıon Technologies, Middle East Technical University** by,

Prof. Dr. Naci Emre Altun
Dean**, Graduate School of Natural and Applied Sciences** ________________

Prof. Dr. Zuhal Akyürek
Head of the Department, **Graduate School of Natural and Applied Sciences** ________________

Assoc. Prof. Dr. Koray K. Yılmaz
Supervisor, **Geodetic and Geographic Information Technologies, METU** ________________

Prof. Dr. M. Lütfi Süzen
Co-Supervisor, **Geological Engineering, METU** ________________

Examining Committee Members:

Assoc. Prof. Dr. Meltem Şenol Balaban
City and Regional Planning, METU ________________

Assoc. Prof. Dr. Koray K. Yılmaz
Geological Engineering, METU ________________

Prof. Dr. M. Lütfi Süzen
Geological Engineering, METU ________________

Prof. Dr. M. Tuğrul Yılmaz
Civil Engineering, METU ________________

Assoc. Prof. Dr. Bedri Kurtuluş
Geological Engineering, Muğla Sıtkı Koçman Üniversitesi ________________

Date: 04.09.2024

I hereby declare that all information in this document has been obtained and presented in accordance with academic rules and ethical conduct. I also declare that, as required by these rules and conduct, I have fully cited and referenced all material and results that are not original to this work.

Name Last name : Ben Forsyth

Signature :

ABSTRACT

A COMPARISON OF SENTINEL 1 AND SENTINEL 2 IMAGE CLASSIFICATION FOR DETECTION OF WATER BODIES IN TURKIYE AND WORLD-WIDE

Forsyth, Ben
Master of Science, Geodetic and Geographic Information Technologies
Supervisor : Assoc. Prof. Dr. Koray K. Yılmaz
Co-Supervisor: Prof. Dr. M. Lütfi Süzen

September 2024, 100 pages

This thesis explores the use of Synthetic Aperture Radar (SAR) and optical remote sensing technologies to monitor and analyze the water extents of various lakes, with a primary focus on Lake Tuz in Turkiye. Employing the Random Forest Classifier, the study classifies land cover types and detects water extents, demonstrating that machine learning techniques maintain consistently high classification accuracy and water monitoring capabilities for Sentinel-1 data. However, the same techniques did not prove as robust when applied to Sentinel-2 data, showing the advantages of SAR over optical data in detecting water bodies under varying atmospheric conditions.

The research shows the significant impact of seasonal changes in water extent on global water resources, with notable seasonal declines and increases in water extent.

The Random Forest Classifier was trained iteratively on multiple regions of interest to enhance classification accuracy and adapt to diverse geographical conditions. The results indicate that the integration of SAR and optical data, coupled with machine learning algorithms, presents a powerful tool for environmental monitoring. Sentinel-1 data showed high overall accuracy in water classification, while Sentinel-

2 data faced challenges due to cloud cover and spectral similarities between different land cover types, resulting in lower overall accuracy. These findings emphasize the potential for remote sensing technologies to enhance our understanding of climate change impacts and aid in the development of effective water resource management strategies.

Keywords: Sentinel-1, Sentinel-2, Lakes, Random Forest Algorithm, Remote Sensing

ÖZ

TÜRKİYE VE DÜNYA ÇAPINDAKİ SU KÜTELLERİNİN TESPİTİNDE SENTINEL 1 VE SENTINEL 2 GÖRÜNTÜ SINIFLANDIRMALARININ KARŞILAŞTIRILMASI

Forsyth, Ben
Yüksek Lisans, Jeodezi ve Coğrafi Bilgi Teknolojileri
Tez Yöneticisi: Doç. Dr. Koray K. Yılmaz
Ortak Tez Yöneticisi: Prof. Dr. M. Lütfi Süzen

Eylül 2024, 100 sayfa

Bu tez, Türkiye'deki Tuz Gölü başta olmak üzere çeşitli göllerdeki su miktarını izlemek ve analiz etmek için Sentetik Açıklıklı Radar ve optik uzaktan algılama teknolojilerinin kullanımını araştırmaktadır. Rastgele Orman Sınıflandırıcısı (RFC) kullanılan bu çalışmada, arazi örtüsü türlerini sınıflandırılarak su alanları tespit edilmektedir. Sonuçlar makine öğrenimi tekniklerinin, Sentinel-1 verileri için sürekli olarak yüksek sınıflandırma doğruluğunu ve su izleme yeteneklerini sağladığını göstermektedir. Bununla birlikte, aynı teknikler Sentinel-2 verilerine uygulandığında performansın daha düşük olduğu sonucuna varılmıştır. Bu durum da değişen atmosferik koşullar altında su kütlelerinin tespitinde SAR'ın optik verilere göre avantajlarını göstermektedir.

Araştırma, su miktarındaki kayda değer mevsimsel düşüşler ve artışlarla birlikte iklim değişikliğinin küresel su kaynakları üzerindeki önemli etkisini gösteriyor.

Rastgele Orman Sınıflandırıcısı, sınıflandırma doğruluğunu geliştirmek ve farklı coğrafi koşullara uyum sağlamak için birden fazla çalışma alanı üzerinde yinelemeli olarak eğitildi. Sonuçlar, SAR ve optik verilerin entegrasyonunun, makine öğrenme algoritmalarıyla birleştiğinde, çevresel izleme için güçlü bir araç sunduğunu göstermektedir. Sentinel-1 verileri, su sınıflandırmasında yüksek genel doğruluk gösterirken, Sentinel-2 verileri, bulut örtüsü ve farklı arazi örtüsü türleri arasındaki spektral benzerlikler nedeniyle zorluklarla karşı karşıya kaldı ve bu da daha düşük genel doğruluk ile sonuçlandı. Bu bulgular, uzaktan algılama teknolojilerinin iklim değişikliğinin etkilerini daha iyi anlamamızı ve böylece daha etkili su kaynakları yönetimi stratejilerinin geliştirilmesine yardımcı olma potansiyelini vurgulamaktadır.

Anahtar Kelimeler: Sentinel-1, Sentinel-2, Göller, Rastgele Orman Algoritması, Uzaktan Algılama

This thesis is dedicated to my family and friends

ACKNOWLEDGMENTS

First of all I would like to express my gratitude to my supervisor Assoc. Prof. Dr. Koray K. Yılmaz and co-supervisor Prof. Dr. M. Lütfi Süzen for their guidance, support and insight throughout this work.

I want to give a special thank you to my mum Lorraine Cameron, Holly and the rest of my family for all their support.

I would also like to extend my gratitude to my friends Atabay Mahmudov, Egemen Göver and El Gato.

A final big thank you to Selin Güzel for all her love and encouragement throughout this endevour. She is the funniest person I've ever met and has been a shining light throughout this process.

TABLE OF CONTENTS

LIST OF TABLES

LIST OF FIGURES

FIGURES

LIST OF ABBREVIATIONS

ABBREVIATIONS	
RF	Random Forest
RFC	Random Forest Classifier
SAR	Synthetic Aperture Radar
VV	Vertical Vertical
VH	Vertical Horizontal
DW	Dynamic World
GCP	Ground Control Points
ROI	Region of Interest
GRD	Ground Range Detected
DEM	Digital Elevation Model
RS	Remote Sensing
CART	Classification and Regression Trees
GEE	Google Earth Engine
NDWI	Normalized Difference Water Index
NDBI	Normalized Difference Built-up Index
NDVI	Normalized Difference Vegetation Index
OA	Overall Accuracy
PA	Producer’s Accuracy
RGB	Red Green Blue

CHAPTER 1

INTRODUCTION

1.1 Remote Sensing on Water Bodies

Most of Earth's surface is covered by water, making it a significant topic of interest (Wang et al. 2011). Water bodies, including lakes, rivers, and reservoirs, play a vital role in sustaining life and maintaining ecological balance. They provide habitat for numerous species, support agriculture, and are essential for human consumption and industrial activities. However, these water bodies are under constant threat from anthropogenic activities and natural phenomena. Climate change, pollution, over-extraction, and land use changes are some of the primary factors contributing to the degradation of water resources.

Productive and ecologically diverse ecosystems thrive along these water bodies, but their extent is shrinking at alarming rates each year (Huang et al. 2018). Accurate assessment and analysis of the spatial extent of water bodies over time are crucial for monitoring the effects of climate change and understanding its impact on the environment, ecology, and water resources. Remote sensing applications are widely used for these analyses due to their advantages, such as broad observation areas, short observation periods, and easy acquisition of necessary information from areas of interest (Fu et al. 2007).

The application of remote sensing technologies, particularly synthetic aperture radar (SAR), has revolutionised the way we monitor and manage water resources. Unlike traditional methods that rely on ground-based observations, remote sensing provides a comprehensive and synoptic view of large areas, enabling continuous monitoring and assessment. SAR systems have demonstrated their capabilities for numerous

Earth observation applications (Krieger et al. 2010) by providing high-resolution two-dimensional images that are unaffected by daylight, cloud coverage, and various weather conditions (Moreira et al. 2013). Additionally, they are highly sensitive to open water, making them valuable for water surface detection (Huang et al. 2018). The Copernicus Sentinel-1 mission is designed as a two-satellite constellation. Each satellite utilises synthetic aperture radar to provide an all-weather, day-and-night supply of imagery of Earth's surface. Sentinel-1, equipped with a C-band SAR sensor, offers effective capabilities for water resource monitoring, however, it requires more complex preprocessing steps, such as speckle filtering, geometric correction, and radiometric calibration, to obtain accurate and usable data. On the other hand, Sentinel-2, which provides multispectral optical imagery, is more straightforward to process due to its simpler atmospheric correction and radiometric calibration procedures. Nevertheless, Sentinel-2's performance can be significantly hindered by cloud cover, which obstructs the view of the Earth's surface, limiting its effectiveness in continuous monitoring.The integration of SAR with other remote sensing technologies has opened new avenues for the detailed monitoring of water bodies, providing critical data for environmental management and policy-making.

In recent years, significant advancements have been made in the field of remote sensing, enhancing the accuracy and efficiency of water body monitoring. The integration of machine learning algorithms with remote sensing data has further improved the classification and analysis of water bodies. Classification methods such as Random Forest (RF) classifiers and Support Vector Machines (SVM) have been widely adopted for their robustness and high accuracy in handling complex and large datasets (Bayik et al. 2018).

1.2 Purpose and Scope of this Study

This thesis aims to explore the application of SAR and machine learning techniques in the classification and monitoring of water bodies. By using the capabilities of SAR and the computational power of machine learning algorithms, this research seeks to develop a reliable and efficient methodology for water surface detection and monitoring. The study focuses on the use of Sentinel-1 and Sentinel-2 satellite imagery to classify and monitor water bodies in various regions, with a particular emphasis on Lake Tuz in Turkiye.

Lake Tuz, Turkiye's second-largest lake and largest saline lake, has been experiencing significant changes in its water extent due to climate change and human activities (Aydin et al. 2020). The dynamic nature of this lake, influenced by seasonal variations and anthropogenic factors, makes it an ideal case study for the application of advanced remote sensing techniques. By analysing the temporal changes in Lake Tuz's water extent using Sentinel-1 and Sentinel-2 data, this research aims to provide valuable insights into the effectiveness of optical and SAR data in water body monitoring.

The study employs a Random Forest (RF) Classifier to process and classify the satellite images, iteratively training the model on multiple regions of interest (ROIs) to enhance classification accuracy. The integration of Sentinel-1 and Sentinel-2 data enables a comprehensive analysis of the lake's temporal changes, demonstrating the strengths and limitations of each data source. Furthermore, the use of Google Earth Engine (GEE) for data processing and analysis facilitates the handling of large datasets and the implementation of complex algorithms.

In addition to Lake Tuz, the research includes other lakes around the world to train the RF classifier progressively. This approach will help in understanding the generalisability of the methodology across different geographical and climatic conditions. By comparing the classification results of various lakes, the study aims to identify the factors influencing the accuracy and reliability of SAR-based water body monitoring.

The findings of this research will contribute to the existing knowledge on remote sensing applications in water resource management, providing a framework for future studies and practical implementations. The developed methodology can be applied to other regions and water bodies, supporting the global efforts in monitoring and managing water resources in the face of climate change and increasing human pressures.

In summary, this thesis investigates the use of SAR and optical data in conjunction with machine learning techniques for the classification and monitoring of water bodies, with a focus on Lake Tuz and other selected lakes world-wide. The research aims to demonstrate the capabilities of SAR in providing accurate and timely data for water surface detection, contributing to the sustainable management of water resources and the mitigation of climate change impacts.

CHAPTER 2

LITERATURE REVIEW

2.1 Causes of Diminishing Water Extent of Lakes

2.1.1 International Lakes

In South America, lakes Titicaca and Poopó are currently found to be shrinking due to climate change. A study by Rodrigo Abarca-Del-Rio et al. (2012) investigates the hydrological relationship between Lake Titicaca and Lake Poopó over the period from 2000 to 2009. Through the use of satellite altimetry and The Moderate Resolution Imaging Spectroradiometer (MODIS) data, the study indicates that the primary source of water level variability in Lake Poopó is not solely Lake Titicaca. Instead, other factors such as increased temperatures, greater evaporation rates, increased glacier and snow melting in the Andes, and higher anthropogenic water usage along the Desaguadero River play significant roles. This shift in hydrological dynamics poses a risk to the already fragile Poopó system, with potential collapse threatening regional water supplies and socioeconomic stability. Further findings indicate that annual evaporation in Lake Poopó has increased significantly due to rising mean annual temperatures, particularly during the rainy season. This trend has then caused reduced inflows during the dry season, affecting the overall balance of the hydrology. In contrast, Lake Titicaca does not show significant changes in its water balance components, highlighting the distinct impacts of climatic variability on each lake (Lima-Quispe et al. 2021).

Another lake that has seen significant water loss over the past decades is lake Mead in the USA, with a 71% decline in water volume from 2000 to 2022 (Hannoun and

Tietjen 2022). According to Wu et al. (2023), who used hierarchical clustering, periods of drought can be split into three periods: early drought (1935-1937), non-drought (1938-2008), and recent drought (2008-2020). The study further utilised scatterplots to understand the historical data and developed predictive models based on linear fitting and breakpoint regression to anticipate future changes. They find that the results from these models indicate that Lake Mead's water levels are expected to follow a decreasing trend with periodic fluctuations due to rainfall and potential reduced water use. Despite the robust methodologies used, the study used annual minimum and maximum water levels instead of more granular monthly data, which may have resulted in some loss of detailed information.

2.1.2 Lakes in Turkiye and the Middle East

Firatli et al. (2022) performed a study spanning 35 lakes that aimed to create a comprehensive national database of these lakes to aid decision-makers in managing these vital water resources. Notable lakes, such as Van Lake, Tuz Lake, Burdur Lake, and Beyşehir Lake, were individually analysed and found to indicate that human activities, such as excessive water withdrawal for irrigation and industrial purposes, significantly impact the surface areas of these lakes. Additionally, the study observes a general trend of decreasing lake areas over the long term, with climate change contributing to these changes through increased temperatures and evaporation rates.

A study by Dervisoglu et al. (2022) spanning from 1985 to 2020 utilized Landsat and Sentinel-2 data to find that Lake Burdur in Turkiye had shrunk significantly over the analysed 35 years, with human activities playing a significant role. By using water indices calculated from satellite imagery, the researchers were able to effectively distinguish between water and non-water areas. The construction of dams and reservoirs for agricultural irrigation has reduced the overall waterflow to the lake even as precipitation levels remain relatively stable. This diversion of water sources during the dry season, along with increased evaporation rates due to rising global temperatures, has further increased the loss of water from the lake. This research highlights the importance of integrating remote sensing data with ground-based observations in order to effectively manage environmental changes. Another study used Landsat satellite images from 1985, 2000, and 2015 to analyse the temporal changes in Lake Burdur's coastline. The findings revealed that the lake area decreased by 70 km², approximately 33.82%, over three decades (Bozdag et al. 2017).

Peker (2019) investigates the variations of the water extent of 16 lakes in Turkiye from 1984 to 2018, google earth engine was utilised along with satellite imagery from Landsat and Sentinel-2. The Normalised Difference Water Index (NDWI) was employed to delineate water extents, which were then compared to in-situ lake level measurements to validate the accuracy. The analysis revealed that lake extents obtained from remote sensing generally correlated well with in-situ measurements, although the correlation coefficients varied between 0.04 and 0.93. The study also found significant relationships between lake extents and meteorological variables, showing positive correlations with precipitation and negative correlations with evaporation.

Lake Tuz is a closed basin lake with a water depth of roughly 1-2m and due to its shallow depth, summer months see an extremely high evaporation rate as water dries up, leaving behind large areas of crusty salt. The total protected area of the Lake Tuz basin covers 7,414 km^2 with water normally covering 1831 km^2 (Dengiz et al. 2010). Yagmur et al. (2021) examines the changes in surface areas of natural lakes within the Konya Closed Basin in Turkiye for long-term (1985-2018) and short-term (2017-2018). The study categorised 18 lakes into saline, freshwater, and brackish groups and analysed their surface area changes using Landsat 5,8 and Sentinel-1,2 satellite images. For long term analysis it was found that while the surface areas of freshwater lakes remained relatively stable, the surface areas of saline lakes, particularly Lake Tuz, significantly decreased by 32%. For the short-term analysis, the findings revealed that Lake Tuz experienced considerable seasonal variability in its surface area due to factors like evaporation and water extraction for salt production, with surface areas shrinking during the summer months. Conversely, Beysehir Lake (fresh water) showed minor fluctuations, indicating a relatively balanced water budget influenced by higher precipitation and regulated water use for drinking and irrigation. This shrinkage over time is backed up by Aydin et al. (2020) who found that Lake Tuz experienced a significant reduction in its water-covered area between 1985 and 2016, primarily due to prolonged droughts from 2001 to 2013, increased temperatures, and excessive groundwater withdrawals. These factors led to a substantial increase in salt-covered areas. The analysis revealed a strong negative correlation between the lake's water levels and climatic indices such as the Standardised Precipitation Index (SPI) and Erinç Aridity Index (EAI).

Another study on Lake Tuz by Aydin-Kandemir and Erlat (2023) investigates the relationship between the salt-covered area of Lake Tuz in Turkiye and its groundwater storage as indicators of drought. This study took place over a 36-year period between 1985 and 2021 with the authors employing various remote sensing techniques, such as Landsat imagery, Gravity Recovery and Climate Experiment data, to analyse changes in the salt-covered area and groundwater storage. The results revealed that a significant expansion of the salt-covered area correlates with a marked decrease in groundwater storage. This relationship shows the impact of not just prolonged drought conditions, but also the impact on the hydrology and ecology in the region due to increased human activities. It is highlighted that the expansion of the salt-covered area is a reliable indicator of reduced groundwater storage and prolonged drought conditions, meaning this correlation serves as a valuable tool for monitoring and managing water resources in arid and semi-arid regions. In order to mitigate the adverse effects of drought and help aid the long-term sustainability of Lake Tuz's ecosystem, the necessity for sustainable water management practices with incorporated remote sensing data is also further emphasised.

Furthermore, Lake Urmia, an endorheic salt lake in northern Iran, has been regressing for multiple decades now. The degradation of the lake is due to multiple factors such as climate change, prolonged drought, reduced rainfall, and human activities including dam construction and excessive water diversion. These actions have caused significantly lower water levels causing higher salinity. This has ended up resulting in the loss of biodiversity, soil erosion, and increased dust storms in the region. A study by Hassanzadeh et al. 2012 utilises a System Dynamics (SD) model, simulating the lake's water balance, considering variables such as inflows, evaporation, and human activities like dam construction and water overuse. The model revealed that changes in inflows due to climate change and excessive surface water usage accounted for 65% of the lake's decline, dam construction contributed 25%, and reduced precipitation had a 10% impact. The study emphasises the critical role of water management policies and proposes that the SD model can serve as a decision-support tool for future interventions. In addition, Rokni et al. 2014 researches the spatiotemporal changes of Lake Urmia, over the period from 2000 to 2013. The research employed various satellite-derived indices, such as the normalised difference water index (NDWI), Modified NDWI (MNDWI), and others, to extract and analyse surface water features from Landsat imagery. The study found the NDWI to be superior for water feature extraction and used it to monitor the drastic decrease in Lake Urmia's surface area. The research also introduced a new approach based on Principal Components of multi-temporal NDWI for detecting changes in the lake's surface water. Results indicated a significant reduction in the lake's surface area, particularly between 2010 and 2013, when the lake lost about one-third of its surface area compared to 2000.

2.2 Limitations of Optical Data and Advantages of SAR

The role that remote sensing plays in water detection has become vital in recent decades. According to Huang et al. (2018), using optical sensors can provide spatially explicit and temporally frequent observational data. Unlike traditional in situ measurements. By utilising this technology, the detailed mapping of water bodies at regional and global scales, and the frequent monitoring of their dynamics over time can be performed. This has led to optical sensors being widely adopted due to their high data availability and suitable resolutions. An example of an optical sensor satellite would be Sentinel-2, built by the European Space Agency with the first launch of Sentinel-2A taking place in 2015 and Sentinel-2B in 2017. Sentinel-2 has bands operating at a spatial resolution 10m, 20m and 60m with RGB bands being 10m. The temporal resolution of a single satellite is 10 days but including the whole constellation brings it down to 5 days (Drusch et al. 2012). The Copernicus program operating and handling Sentinel data has ultimately provided accurate, frequent data and made it incredibly efficient and cost effective to use. Sentinel-2 bands are shown in the table below.

Table 2.1. Sentinel-2 Bands

Band	Central Wavelength (nm)	Bandwidth (nm)	Spatial Resolution (m)
B1 – Coastal Aerosol	443	20	60
B2 – Blue	490	65	10
B3 - Green	560	35	10
B4 - Red	665	30	10
B5 - Visible and Near Infrared	705	15	20
B6 - Visible and Near Infrared	740	15	20
B7 - Visible and Near Infrared	783	20	20
B8 - Visible and Near Infrared	842	115	10
B8A - Visible and Near Infrared	865	20	20

Table 2.1 (continued). Sentinel-2 Bands

B9 – Water Vapor	945	20	60
B10 – Short Wave Infrared (Cirrus)	1375	30	60
B11 - Short Wave Infrared	1610	90	20
B12 - Short Wave Infrared	2190	180	20

When it comes to cloud cover, this can pose a serious problem for image acquisition, as with optical imagery it can lead to obscured, altered or even missing data. The development of synthetic aperture radar mitigates the problems of atmospheric conditions that hinder the acquisition of optical data, and instead allow data to be acquired regardless of cloud cover (Ge at al. 2019). Through proper selection of the operating frequency, radar can penetrate clouds, haze, rain and fog allowing for operation of SAR in unfavourable weather conditions where optical imagery would not be suitable (Ulaby 1981). Furthermore, SAR is also independent of illumination source as it is classified as an active sensor meaning that it provides its own source of illumination. This allows SAR to operate during day or night as it is able to illuminate with variable look angle and wide area coverage. (Chan and Koo 2008).

The synthetic aspect of SAR is related to the spatial resolution and the ratio of the sensor's wavelength to the antenna. An antenna of 4250 metres would be required to obtain a special resolution of 10 metres for a satellite operating at 5 centimetres wavelength. Instead, SAR obtains a sequence of acquisitions from a shorter antenna and combines them. The use of radar in this manner is more sensitive to surface characteristics such as roughness and moisture (Flores-Anderson et al. 2019). Sentinel-1 data utilises synthetic aperture radar imagery which has shown its ability countless times in detecting water on earth independent of daylight or cloud cover. Sentinel-1 operates on C-band which has a wavelength of 3.8-7.5cm and a frequency of 4-8 GHz, it has mild penetration capabilities and exhibits good performance at differentiating water for surrounding areas (Xie et al. 2023).

Abdikan et al. (2016) investigates the use of Sentinel-1 Synthetic Aperture Radar (SAR) imagery for land cover mapping in Istanbul, Turkiye using dual-polarisation (VV and VH) Interferometric Wide swath mode data. The data was processed using a Support Vector Machines (SVM) method for supervised pixel-based image classification, with training and test data sourced from high-resolution Google Earth images. The study found that combining VV and VH polarizations significantly improved the overall classification accuracy to 93.28%, compared to 73.85% and 70.74% when using only VV or VH, respectively. It was observed that using dual-polarimetry not only enhanced the classification accuracy but also facilitated the clear extraction of water and urban classes, despite some misclassifications in hilly areas.

2.3 Image Classification of Satellite Data

2.3.1 Machine Learning Applications for Remote Sensing Based Landcover Classification

Elwan et al. (2022) performed irrigation mapping of SAR images using support vector machines (SVMs). This involved the use of Sentinel-1 and Sentinel-2 data, pre-processing the images and splitting the data into testing and validation data. The training and validation of the data took place at two test sites, the highest overall accuracy (90%) was obtained when the training and validation data was done based on the same test site. The lowest overall accuracy was found when training data was taken from a different test site to that of the validation data (60%).

2.3.2 Random Forest applications for Remote Sensing Based International Landcover Classification

The detection and monitoring of water in lakes plays a crucial role in understanding the impacts of climate change on our ecosystems. In recent years, there has been a growing recognition of the importance of utilising machine learning models to help produce decision-making processes for water management practices. Various classification techniques have been used for detecting and monitoring changes in land use/land cover, such as supervised classification methods (Hua 2017). One popular and effective approach is the use of the random forest classification algorithm. Random forest classification has been widely applied in land cover classification studies and has shown accurate results in these remote sensing tasks. Random forest is particularly favoured for change detection analysis due to its ability to handle large and complex datasets, as well as its robustness in handling noise and uncertainty in the data. In recent years, several studies have successfully employed random forest classification algorithms in water detection as well as monitoring changes in water extent over time. Various remote sensing data and ancillary datasets have been used in these studies, including Sentinel-1 and Sentinel-2 imagery.

Random Forest is an ensemble learning method that operates by constructing a multitude of decision trees during training and outputting the class that is the mode of the classes (classification) or the mean prediction (regression) of the individual trees (Breiman 2001). Random Forests are versatile and can be used for both classification and regression tasks. They are widely used in practice due to their effectiveness, scalability, and ability to handle high-dimensional data. Additionally, they provide a feature importance measure, indicating the relative importance of each feature during the classifier.

Wangchuk and Bolch (2020) present an advanced method for detecting and monitoring glacial lakes in alpine regions using multi-source satellite data and machine learning techniques. By integrating Sentinel-1 Synthetic Aperture Radar (SAR) and Sentinel-2 Multi-spectral Instrument (MSI) data with a random forest classifier model. They were able to address the challenges of mapping glacial lakes, such as small lake size, cloud cover, mountain shadows, seasonal snow, varying turbidity, and frozen surfaces. By using rule-based segmentation of satellite images, the method effectively identifies glacial lake objects and classifies them with high accuracy. The study tested this method across eight alpine regions, demonstrating its robustness and adaptability of the random forest classifier to different geographic and climatic conditions.

The results indicate that the proposed method significantly improves the detection and delineation accuracy of glacial lakes compared to conventional techniques. The random forest classifier model, trained with multi-source data, efficiently differentiates between glacial lake and non-glacial lake objects, minimising errors and reducing the need for manual intervention.

Gislason et al. (2003) explore the application of RFC for classifying multisource remote sensing and geographic data. The RF classifier was compared with other ensemble methods, such as boosting and bagging, using multispectral data from Landsat MSS, elevation, slope, and aspect data in a mountainous area in Colorado. The RF classifier uses a bootstrapping method to create multiple decision trees and evaluates only a random subset of variables at each node, which minimises the correlation between trees and improves classification accuracy.

The results showed that the RF classifier outperformed a single Classification and Regression Tree, with an overall accuracy of 82.8%. The RF classifier was also able to provide valuable insights into variable importance, indicating that elevation and certain spectral bands were crucial for classifying specific land cover types. Additionally, the RF approach was faster in training and classification than boosting, making it a more practical option for large datasets. The study concludes that the RF algorithm is highly effective for land cover classification, offering a good balance between accuracy and computational efficiency.

Fernandez et al. 2022 investigates the changes in the surface areas of Burlan and Pomacochas lakes in Peru from 2014 to 2020. Due to high cloud cover in the region, optical data analysis is challenging, so the study used SAR images from Sentinel-1 A and B processed in Google Earth Engine. The researchers utilised Random Forest, and Support Vector Machine, to classify the images and determine changes in lake contours and surface areas. Additionally, regression methods were used to predict future surface area changes, validated against photogrammetric flight data.

The study found that CART and Random Forest algorithms provided more accurate image classifications, while Support Vector Regression and Random Forest Regression were better suited for regression analysis. The results indicated that both lakes experienced slight increases in area and perimeter during the first months of the year, likely due to increased rainfall. Furthermore, the shapes of the lakes obtained through classification were similar to that of the photogrammetric flight data. The methodology developed in this research offers a rapid and effective approach to classifying SAR images and analysing water body dynamics, which can be replicated in various thematic areas and supports the management of water resources and climate modelling.

2.3.3 Random Forest applications for Remote Sensing Based Landcover Classification in Turkiye

Iban and Sekertekin (2022), investigate the application of various machine learning (ML) methods to map wildfire susceptibility in the Mediterranean region of Turkiye. The study utilised active fire pixels derived from MODIS satellite data to create a wildfire inventory and assessed the performance of seven ML algorithms. Thirteen wildfire conditioning factors, including topographical, meteorological, vegetation, and anthropogenic factors, were used to evaluate the models. The Random Forest algorithm demonstrated the best performance, with an accuracy score of 0.812 and an AUC value of 0.879.

Furthermore, Akar and Güngör (2015), explore the use of the Random Forest classification algorithm enhanced with texture extraction methods and the

Normalised Difference Vegetation Index (NDVI) to improve the detection of tea and hazelnut plantation areas. The study was conducted in the eastern Black Sea region of Turkiye, where tea and hazelnut are significant crops. The authors utilised WorldView-2 satellite images, integrating texture features extracted using the Grey Level Co-occurrence Matrix (GLCM) and Gabor filter with spectral data, to improve classification accuracy. The study found that adding texture information significantly boosted the classification performance of the RF algorithm, with the highest accuracy obtained when using the Gabor filter.

The results showed that the overall classification accuracy improved from 79.05% to 87.89% for summer images and from 71.84% to 79.73% for winter images when texture information was included. The research highlights the effectiveness of combining NDVI and texture methods with the RF algorithm in distinguishing between tea and hazelnut plantations, which have similar spectral reflectance properties and are challenging to differentiate using only spectral data.

2.4 Literature Review Summary

To conclude, this literature review focuses on the adverse effects of climate change on lakes situated in various regions of the globe and how remote sensing techniques can be used to monitor them. There are distinct hydrological dynamics and climate change effects on lakes in South America, as well as the significant water volume decline in Lake Mead, USA, attributable to prolonged drought periods. In Turkiye and the Middle East, lakes such as Van Lake, Tuz Lake, and Lake Urmia showcased the detrimental effects of human activities, climate variability, and increasing evaporation rates, leading to significant surface area reductions and heightened salinity levels. Furthermore, the limitations of optical remote sensing data are discussed, particularly under cloudy conditions, which is then compared to Synthetic Aperture Radar for its ability to penetrate clouds and provide reliable data regardless of atmospheric conditions. The application of machine learning techniques, notably Random Forest, has proven effective in land cover classification and water detection, providing an effective tool for monitoring and managing environmental changes. While previous studies in the literature have primarily focused on using either SAR or optical remote sensing technologies independently to monitor water bodies, this research uniquely integrates both SAR and optical data within a machine learning framework to allow for a comparison of both data sets for water extent classification. Additionally, unlike many studies that concentrate on a single region or lake, this thesis applies its methodology to training a random forest classifier across multiple global lakes, with a special emphasis on classifying Lake Tuz. While providing a more comprehensive analysis of water body dynamics under varying environmental conditions, this study will also showcase the advantages and drawbacks of training a RFC on multiple locations around the world. Furthermore, many studies done in Turkiye, that are also mentioned in this literature review, study lakes over multiple years or decade. This study is more compact and focuses on the analysis of Lake Tuz within one year, providing recent and more detailed insights of the dynamics of the lake in a shorter time span. This work will also add to the research being done in Turkiye, as this study utilises many lakes within Turkiye and applies its unique methodology to locations where this hasn't been done before.

CHAPTER 3

METHODOLOGY

3.1 Study Areas

The main study area is Lake Tuz in Turkiye, with other lakes around the world chosen for progressively training the RFC. The lakes were chosen due to their deteriorating water extents, largely caused by climate change. The region of interest (ROI) of Lake Tuz included the lake and its surrounding area, which partially included Kızılırmak River.

Figure 3.1. Sentinel-2 image of Lake Tuz

Lake Tuz was analysed throughout the year of 2023, with data taken every 12 days. 12-day increments were chosen due to the fact that 12 days is the temporal resolution of Sentinel-1, and Sentinel-2 having a temporal resolution of 10 days, leaving the lowest increment possible being 12 days. In order to draw a comparison between Sentinel-1 and Sentinel-2, RFC was trained on the same ROIs within the same date ranges for both Sentinel-1 and Sentinel-2. The following process was used; first, the RFC was trained on two ROIs and then used to classify a separate ROI. After this, the ROI that was classified would be added to the training data along with the two previously used ROIs, which were then used to classify a new ROI. Subsequently, this ROI that was most recently classified would be added to the collection of training ROIs in order to classify a new ROI and so on. The lakes chosen as ROIs for this process were (Figure 3.2, Figure 3.3, Figure 3.4, Figure 3.5, Figure 3.6):

Lake Burdur – Burdur Gölü (Turkiye): Lake Burdur is a saline lake located in the provinces of Burdur and Isparta.

Lake Egirdir - Eğirdir Gölü (Turkiye): Lake Egirdir is a fresh water lake located in the province of Isparta.

Lake Beysehir – Beyşehir Gölü (Turkiye): Lake Beysehir, a fresh water lake, is located in the province of Konya and is Turkiye's third largest lake.

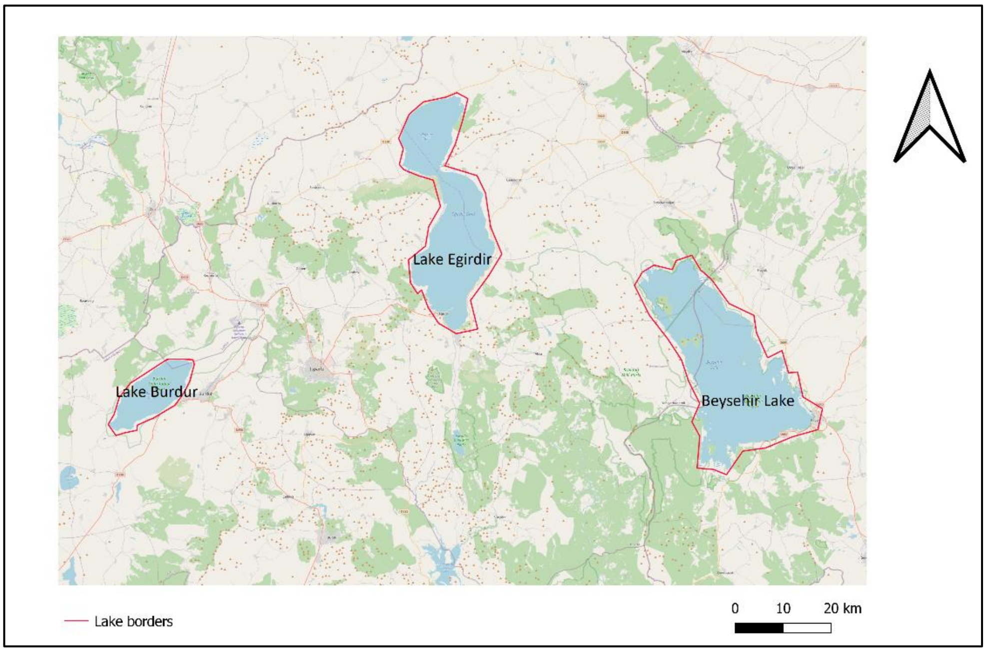

Figure 3.2. Lakes Burdur, Egirdir and Beysehir Outlined

Lake Tuz - Tuz Gölü (Turkiye): Lake Tuz is Turkiye's second largest lake and largest saline lake (Figure 3.3). It is located within the borders of Ankara, Konya and Aksaray provinces and actually provides up to 60% of the total salt production in Turkiye.

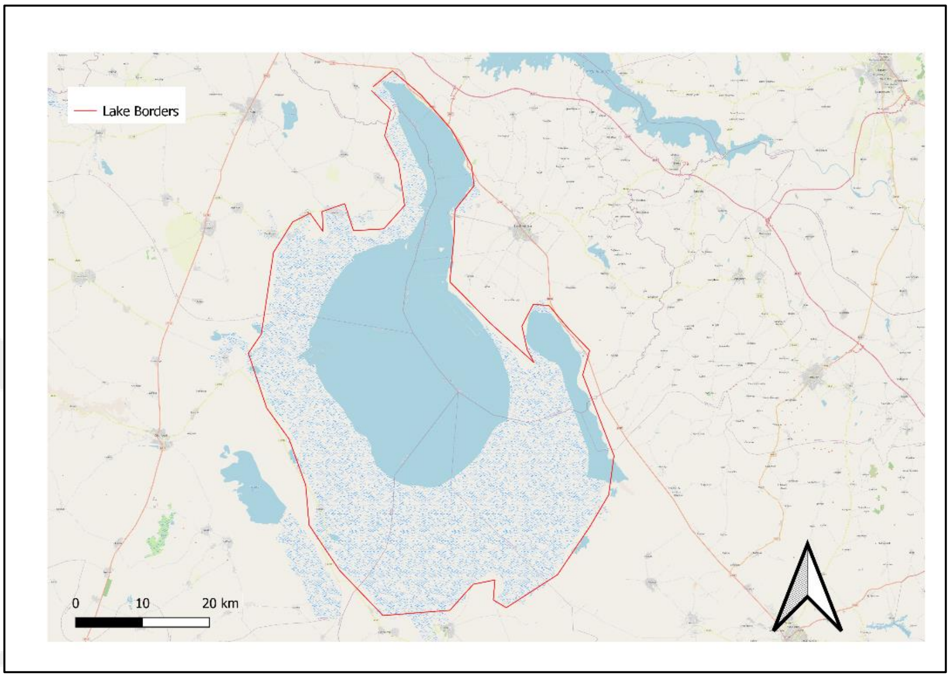

Figure 3.3. Lake Tuz Outlined

Lake Mead (USA): Lake Mead is a reservoir lake formed by hoover dam within the states of Nevada and Arizona.

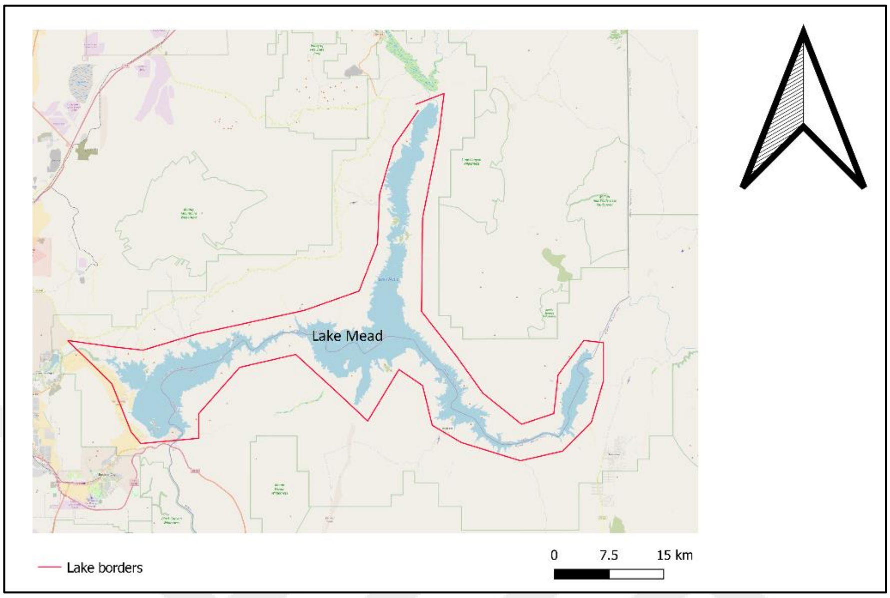

Figure 3.4. Lake Mead Outlined

Lake Titicaca (Bolivia): Lake Titicaca is located on the border between Peru and Bolivia in the Andes mountains. It is the largest lake in South America.

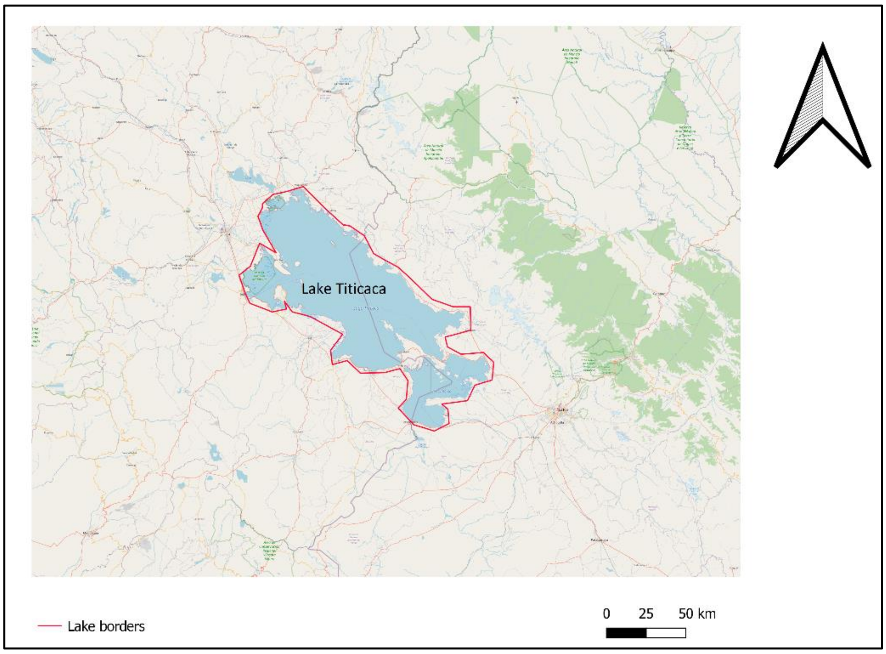

Figure 3.5. Lake Titicaca Outlined

Lake Urmia (Iran): Lake Urmia is a salt lake located between the Iranian provinces of East Azerbaijan and West Azerbaijan.

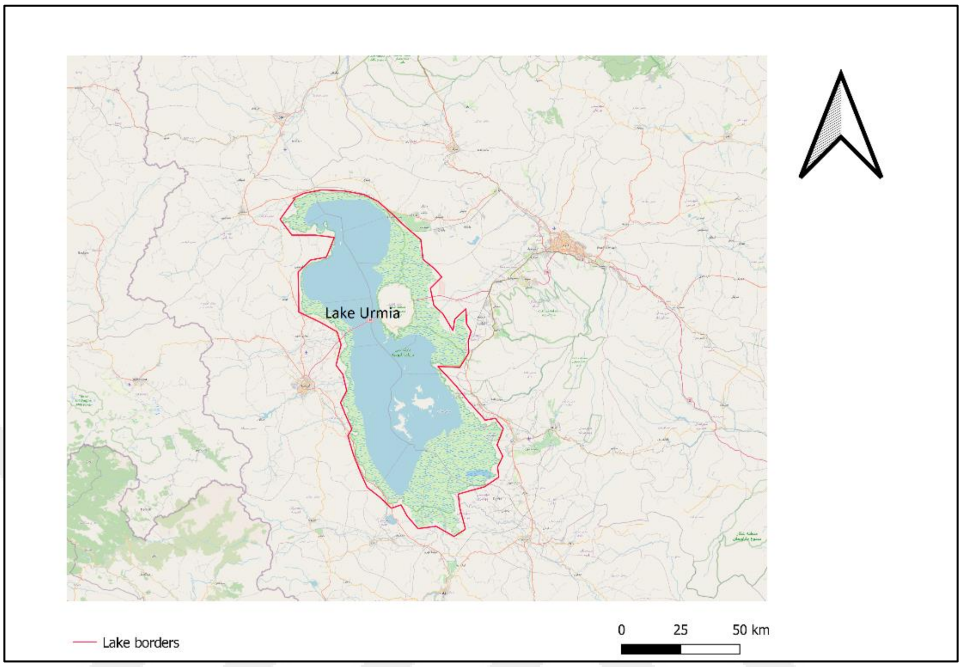

Figure 3.6. Lake Urmia Outlined

The features and characteristics of each lake chosen are shown in Table 3.1.

Table 3.1. Characteristics of each lake chosen for this study

Lake Name	Country	Size (approx.)	Characteristics	Climate	Saline
Lake Beyşehir	Turkey	650 km²	Freshwater lake, tectonic origin, important bird area	Mediterranean	No
Lake Eğirdir	Turkey	482 km²	Freshwater lake, tectonic origin, popular tourist spot	Mediterranean	No
Lake Burdur	Turkey	200 km²	Saline lake, endorheic basin, Ramsar site	Mediterranean	Yes
Lake Tuz	Turkey	1,665 km²	Hypersaline lake, endorheic basin, important salt source	Continental	Yes
Lake Mead	USA	640 km²	Artificial reservoir, Colorado River, recreation area	Arid	No
Lake Titicaca	Peru/Bolivia	8,372 km²	Highest navigable lake, tectonic origin	Highland	No
Lake Urmia	Iran	5,200 km²	Saline lake, endorheic basin, shrinking due to drought	Continental	Yes

While excluding Lake Tuz from training data and attempting to classify it based on other lakes presents a challenge, it's not impossible. The unique hypersaline nature and seasonal variations of Lake Tuz differentiate it significantly from most of the remaining lakes in dataset. However, the diversity of these remaining lakes in terms of size, origin, climate, and location can still provide a basis for classification. The model might leverage variations in salinity among the other lakes and SAR's sensitivity to such changes. To expand on earlier as to why these lakes were chosen to train the RFC, Lake Beyşehir and Lake Eğirdir offer a contrasting freshwater baseline, helping the model learn to distinguish between drastically different salinity levels based on spectral signatures. Lake Burdur provides valuable insights into the spectral behavior of saline water, though less extreme than Lake Tuz. Lake Mead showcases human-induced changes in water bodies, while Lake Titicaca demonstrates the influence of high-altitude environments on satellite imagery such as atmospheric conditions and surrounding terrain. Lastly, Lake Urmia, with its fluctuating water levels and high salinity, provides a glimpse into the dynamic nature of such environments, which may aid in interpreting Lake Tuz's behavior. These factors as well as each lakes susceptibility to climate change and their respective shrinkages over the passing decades made them ideal choices for this study.

First, Lake Egirdir was classified, with the training data being taken from Lake Burdur and Lake Mead, then Lake Beysheir was classified and included the ROIs of Lake Burdur, Lake Mead and Lake Egirdir in the training data. This went process went on with Lake Titicaca, Lake Urmia and Lake Tuz being classified. Table 3.2 shows which ROIs were used during training for which ROI being classified. For Sentinel-1, each ROI contained 40 GCPs and for Sentinel-2 data each ROI contained 100 GCPs. Classification was carried out on these lakes individually in order to monitor the accuracy while continuously adding training data. The dates used to compile images into a single median image for training and monitoring these continuous results were 13/01/23-25/02/23.

Table 3.2 ROI training data used for classification of each ROI

ROI (classified)	**ROI (training data)**
Egirdir	Burdur, Mead
Beysehir	Burdur, Mead, Egirdir
Titicaca	Beysehir, Burdur, Mead, Egirdir
Urmia	Titicaca, Beysehir, Burdur, Mead, Egirdir
Tuz	Urmia, Titicaca, Beysehir, Burdur, Mead, Egirdir

The main purpose of this study is to test the classification accuracies of both Sentinel-1 and Sentinel-2 for detecting water after training the classifier on multiple separate ROIs around the world, with final classification being done on Lake Tuz. Lake Tuz is then monitored throughout 2023 using this compiled training data which is all still based on the dates 13/01/23-25/02/23. The primary classifier used for this study is the random forest classifier due to its use as a reliable and effective alternative to other regular pixel-based classifications and its specific effectiveness at classifying satellite imagery (Bayik *et al.* 2018). For Sentinel-1 data, each ROI contained 40 GCPs and for Sentinel-2 data each ROI contained 80-100 GCPs. For both satellite's data, each class contained 20 GCPs with Sentinel-1 data utilising two classes and Sentinel-2 utilising 4-5 classes depending on the time of year. This process is discussed further in chapter 3.4.1.

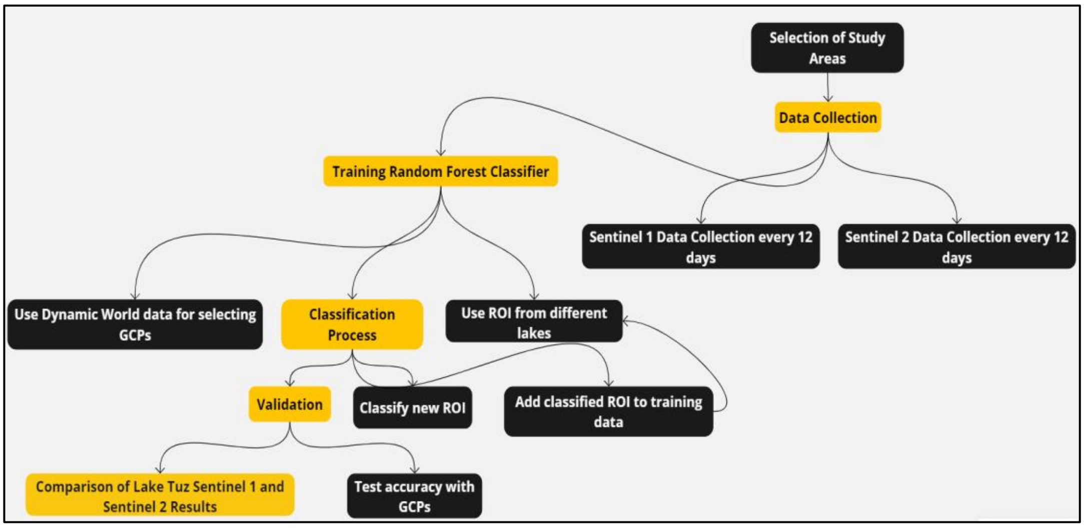

Figure 3.7. Flowchart of Methodology

It is important to note that throughout this whole study, all GCPs used during the training processes and the GCPs used during validation processes are separate and independent from each other in order to provide more reliable accuracy assessments. Training GCPs were based on visual inspection of Sentinel-2 RGB images whereas validation GCPs were based primarily on Dynamic World data as is discussed more in chapter 3.3.

Finally, Lake Tuz was also classified with training data taken from Lake Tuz itself in order to compare the results of classifying when using diversified training data with classifying using training data only from the ROI being classified. This was again done on both Sentinel-1 and Sentinel-2 images, compiling images taken between the dates of 13/01/23-25/02/23 through median filtering to compare the results of using only training data from Lake Tuz with the iterative diverse training data. The 13/01/23-25/02/23 time period was used for both training and classification, the same as done on while increasing training data.

3.2 Data Sets

The Sentinel-1 dataset used in GEE was the S1_GRD image collection; this collection has already gone through pre-processing (Google, 2024). These steps include:

- Having an applied orbit filter which updates orbit metadata with a reconstituted orbit file
- Having a ground range detected (GRD) border noise removal which removes low intensity noise
- Thermal noise removal which removes additive noise in sub-swaths to help reduce discontinuities between sub-swaths
- Application of radiometric calibration values which computes backscatter intensity using sensor calibration parameters in the GRD metadata
- Terrain correction which converts data from ground range geometry, which does not take terrain into account, to σ° using the SRTM 30 meter DEM or the ASTER DEM for high latitudes

All Sentinel-2 data used is 2A level harmonised, which has orthorectified atmospherically corrected surface reflectance. Level-2A data is a Bottom-Of-Atmosphere (BOA) reflectance product created by applying atmospheric correction, terrain and cirrus correction, and scene classification to Level-1C data (Sola et al. 2018).

3.3 Dynamic World

Dynamic World (DW) is a near real time automated approach for classifying land cover globally that is powered by Google Earth Engine. All Dynamic World data utilises 10m 1C Sentinel-2 imagery to train deep learning models for classification (Brown *et al.* 2022). The workflow of DW involves a convolutional neural network, trained on vast amounts of hand-labled imagery and unsupervised learning, analysing the spectral information from Sentinel-2 images. This model then predicts the probability of each pixel belonging to one of nine predefined land cover classes. The system also employs cloud masking techniques to refine classifications and exclude areas obscured by clouds. The final output is a continuously updated global dataset in Google Earth Engine, containing probability maps for each land cover class. This essentially allows users access to an on demand classification portal where users can select there own dates to classify images anywhere in the world, as long as Sentinel-2 data is available during the designated time period and location. The dataset is designed for users to create their own classes for local areas and increase accuracy and efficiency. All dynamic world and Sentinel-2 images used in this study utilise images with cloud cover being less than 20%, with a few exceptions for the regular Sentinel-2 images used in classification which is explained in the later in chapter 3.4.2.

The 9 probability bands for dynamic world data are water; trees; grass; flooded_vegetation as one band; crops; shrub_and_scrub as one band; built; bare and lastly snow_and_ice as one band (Figure 3.8).

Due to a lack of access to ground truth data, Dynamic world data was primarily used as validation for this study, with ground control points being based off of dynamic world data. Dynamic world was chosen for this task of choosing validation GCPs due to the fact it was a reliable and world-wide data set that covered all the study areas chosen for this research. Dynamic World's strengths lie in its near-real-time data updated every few days, allowing for validation against recent land cover changes. This proves particularly valuable for applications requiring timely monitoring, such as what was required in this study. Its global coverage at a high resolution of 10 metres further enhances validation capabilities, capturing fine-grained local changes that coarser datasets might overlook. The dataset also provides probabilities for nine land cover classes, going beyond simple binary classifications to validate more complex land cover maps. Cloud filtering minimises the impact of cloud cover, improving validation reliability, while its own accuracy has been validated against expert-labled data, instilling confidence in its use as a reference. The reported overall agreement between Dynamic World's single-image model outputs and expert labels gave an overall accuracy of 73.8% (Brown *et al.* 2022). In addition, its accessibility made it ideal for this study, Dynamic World is freely available, facilitating wider adoption and reproducibility of research. This removes barriers associated with costly or restricted datasets.

Ultimately it can be used for traditional post-classification accuracy assessments, validating change detection algorithms and refining classification models. Wang et al. (2023) used DW data for validating classification results while studying coastal aquaculture in China. In addition to DW data, visual inspection of Sentinel-2 images was however also used in conjunction with dynamic world data for selecting validation GCPs. Figure 3.8 shows an example of DW classifying Lake Burdur.

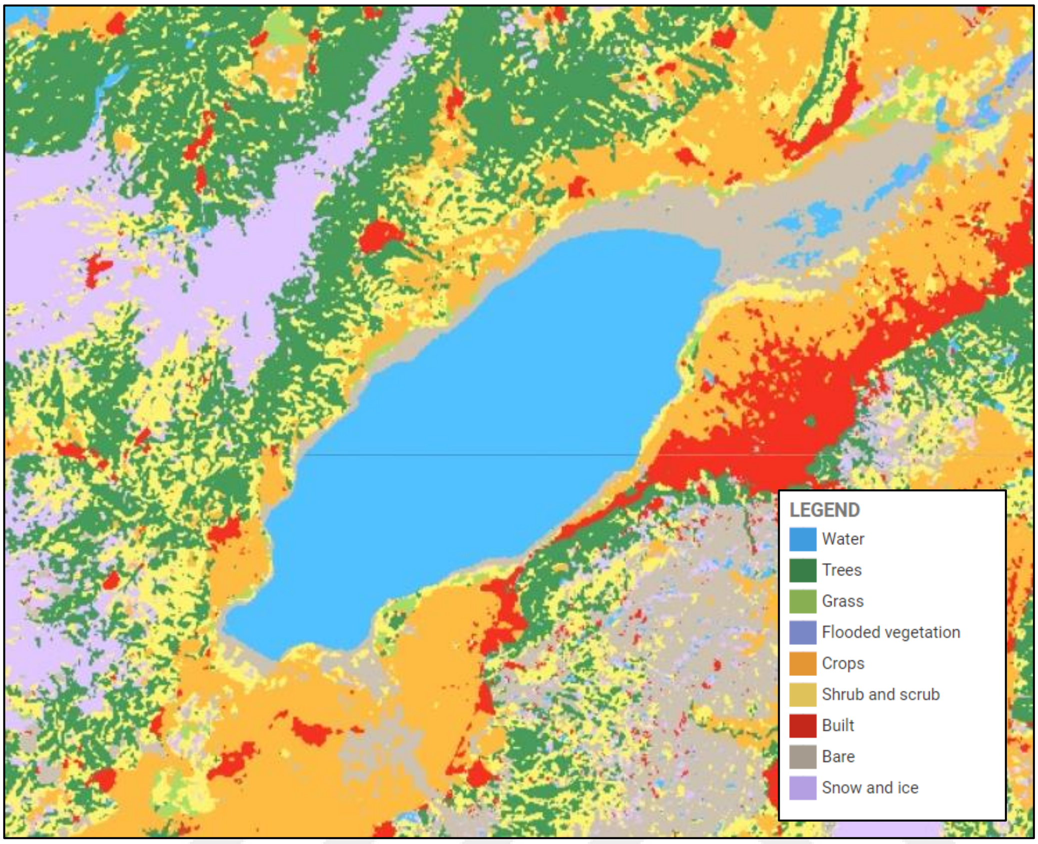

Figure 3.8. Dynamic world layer of Lake Burdur before reclassification

All of the 9 Dynamic world probability bands were reclassified in GEE to match the classes used for this study. This was done by loading an already classified dynamic world layer into GEE, placing 20 new GCPs for each class, both for validation and training based on the 5 classes used for Sentinel-2 classification. 70% of the GCPs were selected randomly for training and the other 30% selected for validation, running RFC to create a new classified layer. This resulted in a dynamic world classification with only 5 classes used for Sentinel-2 in this study, these being Water, Built, Vegetation, Bare and Snow. An example showing the results of the reclassification on Lake Burdur can be seen in Figure 3.9.

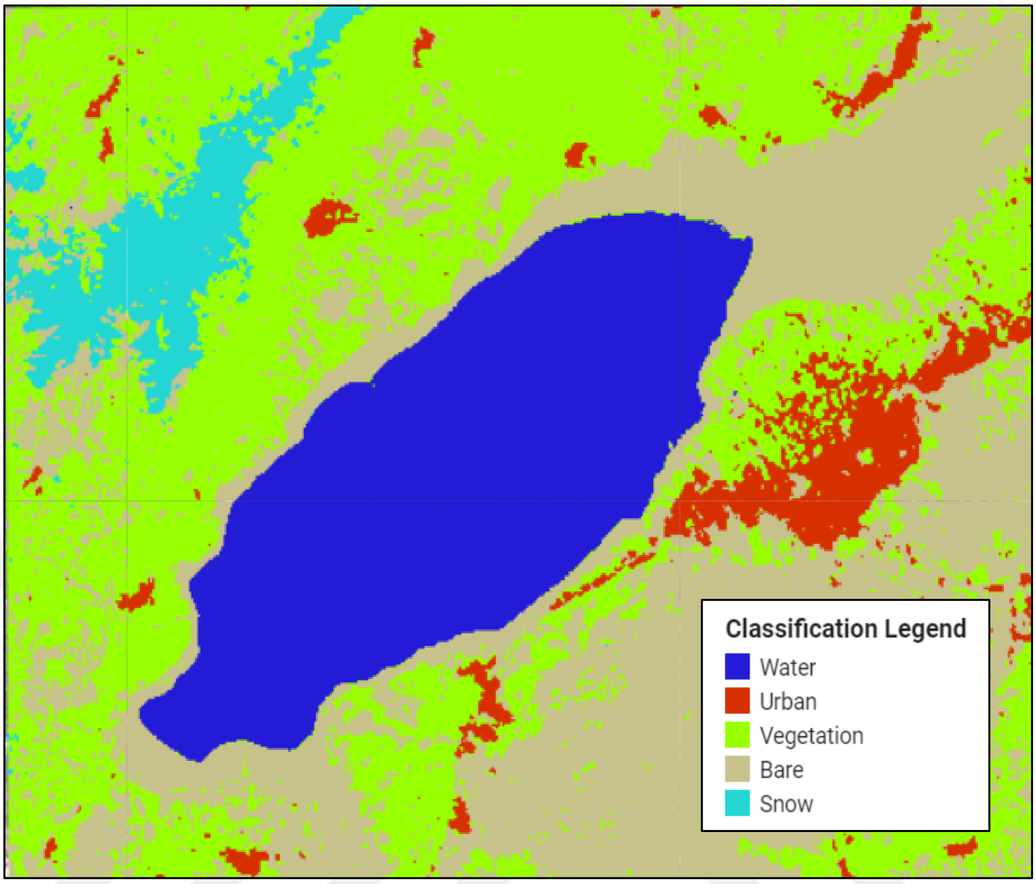

Figure 3.9. Dynamic world layer of Lake Burdur after reclassification

As can be seen in Figure 3.9, the landcover results have been simplified from those in figure 3.8 into 5 classes in order to match that of the classes used in this study. These re-classified layers were constructed multiple times for every lake involved in this study for the purposes of being used as validation data (along with visual inspection) for both Sentinel-1 and Sentinel-2. For Sentinel-1 data, any area that was classified as urban, vegetation, bare or snow in the dynamic world layer was marked as non-water for validation. In figure 3.10 we can see the colours changed to match the classes used for Sentinel 1 data.

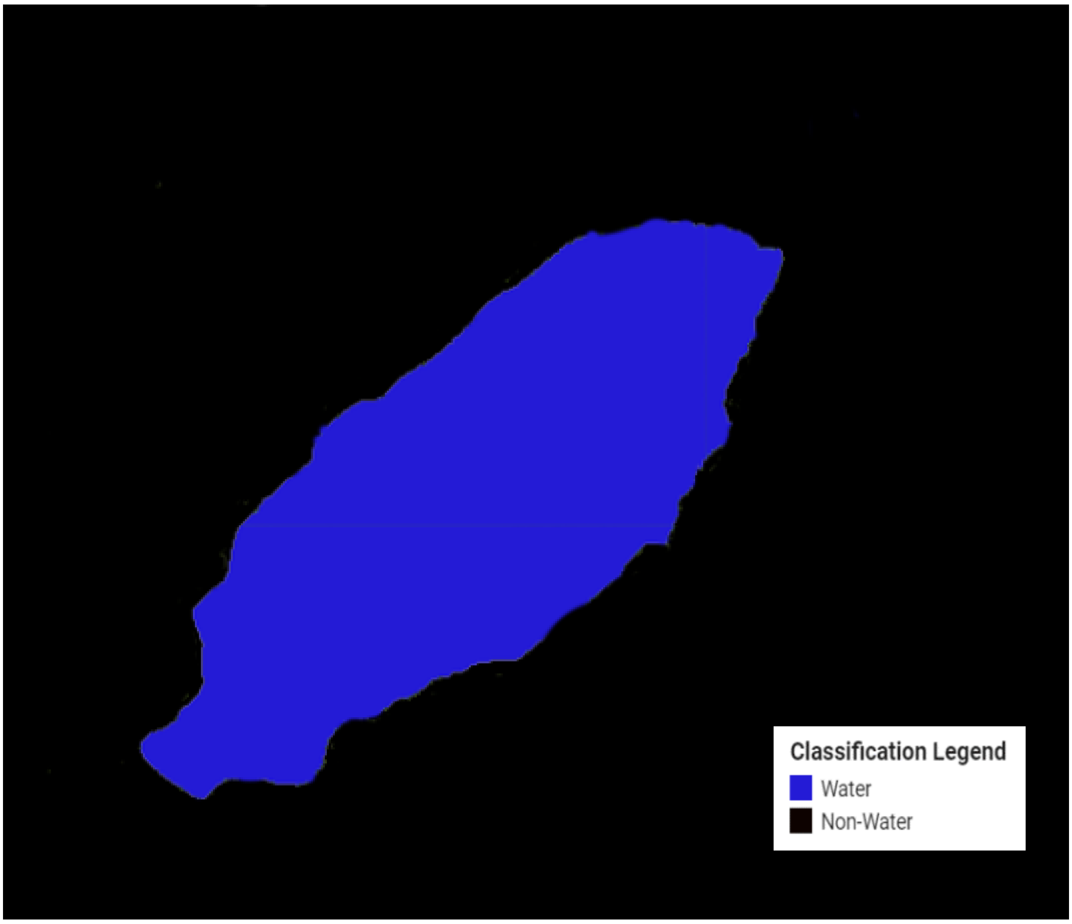

Figure 3.10. Dynamic world layer of Lake Burdur after reclassification for Sentinel-1 classes.

3.4 Classification Procedure

3.4.1 Google Earth Engine

Google Earth Engine (GEE) was the main tool used for all work done on this thesis. It is a powerful, cloud-based platform designed for planetary-scale environmental data analysis. It offers access to a vast repository of satellite imagery and geospatial datasets from sources such as NASA, USGS and ESA. Using Google's cloud computing infrastructure, it can analyse and visualize large-scale datasets, create maps, and generate time-lapse videos. GEE supports custom geospatial analysis via JavaScript and Python APIs, facilitating research and practical applications in fields like environmental monitoring, climate research and agriculture. Additionally, it contains interactive tools for visualising geospatial data and has integration with machine learning frameworks for advanced data analysis and predictive modelling. Its ease of use and range of capabilities made it ideal for this study. It's user interface is seen in figure 3.11.

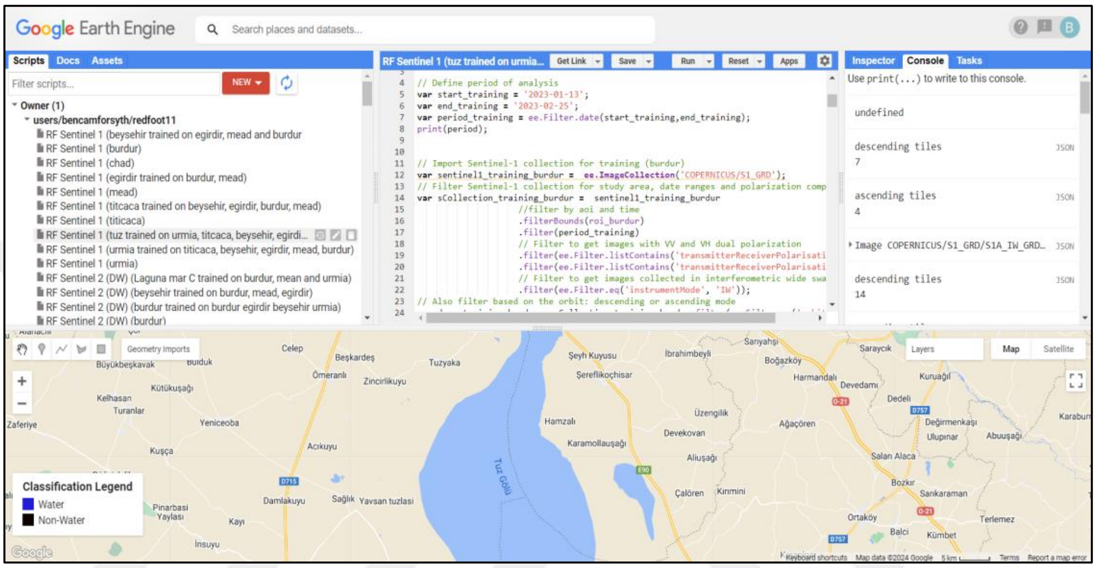

Figure 3.11. User Interface of Google Earth Engine

For selecting the study areas, polygon shapefiles were created over the regions of interest in QGIS using the OSM standard webservice tool. The shapefiles were then imported into google earth engine. GEE was then used for all subsequent image processing of the Sentinel-1 and Sentinel-2 images including filtering, training, classification, accuracy analysis and class area coverage. Aside from selecting study area, every task of for this thesis was carried out using GEE.

3.4.2 Sentinel-2 Classification

The Sentinel-2 images of Lake Tuz were taken over 12 day intervals throughout the year of 2023. Within each 12-day interval, every available Sentinel-2 image was combined using a median filter, in the case of only one image being available then only that image was used. The median filter helps to reduce noise by reducing an image collection by calculating the median of all values at each pixel across the stack of all matching bands where bands are matched by name. Median filters are less sensitive to outliers than mean filters. Additionally, it helps smooth out temporal variations that might occur due to transient phenomena like clouds, shadows, or short-term vegetation changes. By using images from multiple dates, the median composite captures the typical reflectance characteristics of the region over time, which can be more representative of the land cover classes than any single image. Finally median filters preserve the edges of features, which is very important for accurate classification (Quan *et al.* 2020). This method resulted in 30 total images throughout the year. This allows for a yearlong overview of the study areas wherein comparisons between Sentinel-1 classification and Sentinel-2 classification can be done. For selection of the Sentinel-2 images, cloud cover was set to a maximum of 20, meaning that cloud cover was not allowed to take over more than 20 percent of the image. It should be noted however that some 12-day periods, specifically 14/03-25/03, 07/04-18/04 and 19/04-30/04 had to have their cloud coverage allowance increased to 60, with 09/11-20/11 having to have cloud cover increased to 80 as there was no data available with less cloud cover during these periods.

An example of the code for image selection can be seen in figure 3.12.

The classes chosen for this research were groups that would cover all aspects of potential landcover and would encompass other subclasses. The classes for Sentinel-2 were defined as ‘Water’, ‘Built’, ‘Vegetation’, ‘Bare’ and ‘Snow’. Water included all water in an image, built covers all urban areas and man-made objects, vegetation covers all shrubs, forests, agriculture etc., bare land covers any other land that is not covered by another class and snow includes both snow and ice. In the code there is a knowledge filter to filter out the snow class during summer months, this will help improve classification by making sure nothing is misclassified as snow when it is not present in an ROI. Furthermore, latitude information is included in the knowledge filter, so that the snow class' GCPs are excluded for the merging process with other GCPs when the ROI for classification is located in the northern or southern hemisphere's summer. This was necessary due to the summers occurring at different times in the year for each hemisphere.

To do this, a variable is created that retrieves and stores the latitude of the ROI being classified, the latitude information is contained in the metadata of the shapefile of the ROI that was imported from QGIS. If the latitude is found to be greater than 0 then the latitude of the ROI is defined as 'northern', if it is less than 0 then it is defined as 'southern'. Conditions are then set not to merge the snow training GCPs with the rest of the classes during the northern hemisphere summer months with an 'if' statement and again during the southern hemisphere summer months with an 'else if' statement. An 'else' statement is then created to merge snow when the above conditions do not apply, meaning during all other months in both hemispheres snow will be included in the merging process. The same is then done for validation GCPs so that snow GCPs will not be used to validate the classification accuracy during summer months of the ROI. The purpose of this section of code is to provide flexibility of classification areas and allow for classification anywhere in the world by reducing misclassification of a class that is dependent on time of year and hemisphere.

The code allows for a median image to be selected for training, and a separate image to be selected for classification. This means that training the RFC can be done using one time period in one location, and then that can be used to classify another time period at another location.

For the purposes of this study, all areas being classified were separate to that of the areas that the RFC was trained on, resulting in all GCPs at the ROI of classification being used for validation. Subsequently all GCPs at the ROIs used for training were all included in training the RFC. 20 GCPs were selected for each class covering a certain ROI, with 5 classes this means that each ROI has 100 associated GCPs. As Lake Tuz is classified, 6 ROIs are used for training, meaning that 600 GCPs in total are used for training and the 100 GCPs associated with Lake Tuz are used for validation. As the dates defining the ROI being classified were changed, the dates defining the ROIs used for training stayed the same. This ensured that training GCPs were not required to be reselected due to features changing over time, GCPs used for validation were however required to be changed with every 12-day interval. The validation GCPs used for the accuracy assessment were picked based on dynamic world data, essentially using the dynamic world data as validation data as mentioned previously.

After merging all GCPs depending on dates and hemisphere, both the GCPs used for training and the GCPs used for validation were given random values using the 'randomColumn(); function'. All the training GCPs were then overlaid with their respective ROIs by using the 'sampleRegions();' function. This Samples the ROI at the locations of the features in the random column of training GCPs feature collection. Each sampled pixel will have its band values along with the properties of the corresponding feature, in this case, the 'class' property.

This step was repeated for every ROI used in training for classification. All overlayed GCPs were then again merged together and used as a feature for training the classifier.

For Sentinel-2, indices were created for the use as variables for classification, these were NDWI, NDBI and NDVI. These were used to enhance the analysis of satellite imagery by emphasizing specific land surface features by distinguishing between different land cover types. NDVI was used to aid in the classification of water whereas NDVI and NDBI were used to aid in the classification of built and vegetation areas. These indices were created by performing a normalised difference calculation in GEE. The bands are defined as below.

- NDWI is defined as $NDWI = (NIR - SWIR) \div (NIR + SWIR)$ therefore requiring the calculation of $Band\,3 - Band\,8 \div Band\,3 + Band\,8$ for corresponding Sentinel-2 bands in the GEE code.
- NDVI is defined as $NDVI = (NIR - R) / (NIR + R)$ therefore requiring the calculation of $Band\,8 - Band\,4 \div Band\,8 + Band\,4$ in the GEE code for Sentinel-2 data.
- NDBI is defined as $NDBI = (SWIR - NIR) / (SWIR + NIR)$ therefore requiring the calculation of $Band\,11 - Band\,8 \div Band\,11 + Band\,8$ in the GEE code using Sentinel-2 data.

The inclusion of these indices can indirectly help identify areas that might be shadowed. These indices enhance specific features of the image (e.g., vegetation, water bodies, and built-up areas) that can indirectly help mitigate the impact of shadows during analysis. Indices increase the contrast between features of interest such as vegetation or water with shadows, making it easier to differentiate between them during analysis.

Bands used as variables for classification of Sentinel-2 data were B1, B2, B3, B4, B5, B6, B7, B8, B8A, B11, B12 along with NDVI, NDWI, NDBI. Originally, all Sentinel-2 bands were used but B9 and B10 were eliminated as they were found to have relatively low importance values for the RFC according to the classifier explanation.

The random forest classifier is trained using 50 trees meaning that the model consists of 50 decision trees. Each tree is built from a random subset of the training data, and the final prediction is made by aggregating the predictions from all the trees. The usage of more decision trees was tested but it was found to make a negligible difference, thus for the sake of time and resource conservation the smallest number of viable trees was used. All other hyperparameters were left unspecified meaning that they revert to the GEE default.

In this case, default hyperparameters set the number of variables per split to the square root of the number of variables. The number of variables varies depending on the data used, in this case there are 13 variables which include the selected bands along with the spectral indices. The 'class' variable is not an input variable but rather the target variable that the classifier is trying to predict. The square root of the number of variables (13) is approximately 3.6. Since we can't have a fraction of a variable, the number of variables per split would be rounded down to the nearest whole number, which is 3. Rounding down leads to a slightly more conservative approach. However, by considering fewer variables at each split, the algorithm is less likely to overfit the training data, potentially improving its ability to generalise to new, unseen data. Evaluating fewer variables at each split can also lead to some computational savings, particularly for large datasets or when training many trees in the forest (Hastie et al. 2009). In practice, rounding down to the nearest whole number has been shown to work well in many cases. While there might be situations where rounding up could lead to slightly better performance, the difference is often marginal, and the potential benefits of conservatism and computational efficiency outweigh the slight potential gain in accuracy.

Overall, this is considered standard practice as setting the number of variables per split to the square root of the total number of features helps ensure that each tree in the forest is somewhat different from the others, which enhances the diversity of the ensemble and, consequently, its overall performance (Hastie *et al.* 2009). In addition, the minimum leaf population is set to 1 so each leaf node has at least one sample. The bag fraction indicates the fraction of the training data to be used to train each tree, here it is set to 0.5, meaning each tree is trained on a random sample containing 50% of the training data. Finally, the maximum number of leaf nodes has no limit and the randomisation seed is set to 0 to ensure reproducibility. The seed sets the random number generator to a specific state, ensuring that the random sampling and other random processes are the same each time the model is trained (Breiman 2001).

Colours were chosen according to what best fit each class for seamless and clear representation. For Sentinel-2, water was assigned blue, built was assigned red, vegetation was assigned green, bare was assigned brown and snow was assigned light blue.

A focal mode filter was added to the code in order to eliminate single pixels or small misclassified areas. This was given a radius of 3 so the immediate 3 pixels surrounding each pixel would be included in retrieving the mode, secondly the number of iterations were set to 1. This filter was applied to the classified layer, which created a new layer that was added.

Both user’s accuracy and producer’s accuracy are calculated along with overall accuracy. Producer’s is especially important in the determining the accuracies of the classification of each individual class. Producer's accuracy in image classification measures how well a model identifies all instances of a particular class in the validation data. It focuses on the model's ability to avoid false negatives (omissions). To calculate producer's accuracy for a specific class, the number of correctly classified pixels of that class is divided by the total number of pixels that actually belong to that class in the validation data. It's essentially the proportion of actual instances of a class that the model correctly predicted. In the case of this study, it was used for understanding the accuracy of the classification of water for Sentinel-1 and Sentinel-2 images. A confusion matrix was also created in order to understand which classes were being confused with each other.

The total area for each class is also calculated and printed in kilometres squared. This was required for later analysis of the comparison of Sentinel-1 and Sentinel-2 classification. First an image is generated where each pixel value represents the pixel's area in square metres with the classified image added as a band to the area image. The sum of pixel areas is then computed for each class within the ROI at a scale of 10 metres. The reducer groups the sum of pixel areas by the class band and retrieves the list of grouped area results. For each item, a dictionary is created, the class number is extracted, and is divided by 1e6 to convert the calculated area from square meters into square kilometres.

Finally, it is very important to know that when printing the classification layers of Sentinel-2 data all the 'Non-Water' classes were given the same colour representation since the main purpose of this study is water detection. This resulted in Vegetation, Urban, Bare and snow classes being represented as black with Water represented as blue.

3.4.3 Sentinel-1 Classification

For Sentinel-1 data, the same 12-day period dates were chosen with the rest of the procedure for classifying Sentinel-1 images being the same as Sentinel-2 with a few key differences. First of all, only water and non-water (binary data) were chosen as classes. Due to the nature of SAR detecting backscatter due to surface roughness, detecting further types of non-water classes would prove challenging only utilising SAR data. Since water detection is the primary goal of this work, binary data was deemed most appropriate. This means there was also no knowledge filter required to eliminate the snow class depending on certain conditions.

Images were filtered to only collect those in interferometric wide swath (IW) mode which is the main acquisition mode for Sentinel-1 land data and acquires data with a 250 km swath at 5 m by 20 m spatial resolution. This balance between coverage and resolution is beneficial for detailed analysis over large regions. IW mode also supports dual polarisation which is essential for this study, providing additional information about the surface properties and allowing for improved classification and analysis of different land cover types. While studies have found that VV polarisation outperforms VH polarisation in monitoring water levels of features such as reservoirs, providing higher accuracy in delineating water features (Souza *et al.* 2022), the polarisations used for Sentinel-1 data in this study are VV and VH due to the fact these polarisations have proven to be very effective at detecting water (Clement *et al.* 2018). Furthermore, combining VV and VH polarizations in water detection algorithms yields high accuracy (Twele *et al.* 2016). Both ascending and descending tiles with these polarisations were collected with a mean filter applied for each variation. This resulted in 4 different variations of mean filtered images which were VV ascending, VV descending, VH ascending and VH descending. These images are then compiled into a single median image used in the classification process, either for training or classification, with both VV and VH polarisations being used as variables for the random forest classifier. With only 2 variables in use for training the classifier, this means the number of variables considered at each split will be 1. The square root of 2 (the total number of variables) is approximately 1.41. Since we need to round this down to the nearest whole number, the final number of variables per split becomes 1. In practical terms, this means that at each node in each decision tree within the Random Forest, the algorithm will randomly select only one of the two available variables (either VH or VV) to make the splitting decision.

Images for classification were again taken during 12-day intervals throughout the year of 2023 resulting in 30 total images throughout the year. In order to create images of both the training and validation ROIs, median images combining both ascending and descending images were used. This was done to improve spatial coverage and mitigate shadowing and layover effects that are common in SAR imagery. This can also lead to enhanced feature detection as different passes can highlight different features and surface properties (Ferrara *et al.* 2009). Furthermore, as mentioned previously, using a median filter to combine images can reduce noise such as speckle to improve classification.

The selected dates for training the ROIs for Sentinel-1 were the same as Sentinel-2, with the dates used for the training ROIs kept consistent throughout each single classification so that training GCP locations did not need to be changed due to temporal changes of the ROIs. As with Sentinel-2 data, the GCPs were set into random columns, overlayed with their respective ROIs and merged together into either the training GCPs or validation GCPs variable. The training GCPs were used as a feature in training the classifier and the validation GCPs overlaying the ROI being classified were used to assess the accuracy.

As with Sentinel-2 colour selection for class representation, colours were chosen for seamless representation and clarity with water being assigned to blue and non-water being assigned to black. The other hyperparameters of the RFC were set to the same as those when classifying the Sentinel-2 images. A focal mode filter was also applied to the final classified layers using the same parameters of the radius being set to 3 and the number of iterations set to 1. Calculations of the total class areas were also carried out along with overall accuracy, producer's and user's accuracy.

3.5 Methodology Summary

In summary, this study utilised an approach to classify and monitor water extents in various lakes worldwide, with a primary focus on Lake Tuz in Turkiye. The methodology integrated Sentinel-1 and Sentinel-2 satellite imagery, leveraging their respective data characteristics for later comparison of results. The Random Forest Classifier was employed to process and classify the satellite images, iteratively trained on multiple regions of interest to monitor water coverage, accuracy changes and potentially improve it. Data was processed in GEE with the Dynamic World application along with visual inspection being used as a source of validation for selecting validation GCPs. Lake Tuz, being the primary focus of this study, is monitored throughout the year of 2023, observing changes in water coverage throughout the year while utilising the RFC trained on worldwide data. By applying various image processing techniques, such as median filtering and focal mode filtering, the study endeavoured to obtain high-quality classification results. This framework enabled monitoring of water extents, contributing valuable insights into the impacts of seasonal change on water resources in Turkiye as discussed in the next chapter.

CHAPTER 4

RESULTS AND DISCUSSIONS

4.1 Sentinel-1 Results

4.1.1 Increasing Sentinel-1 Training Data

The table below presents the overall accuracy (OA) and producer's accuracy (PA) of water for the image classification of multiple lakes, utilising Sentinel-1 imagery. The lakes analysed include Egirdir, Beysehir, Titicaca, Urmia, and Tuz, with each successive lake classification incorporating (ROIs) from previously classified lakes into its training data. This cumulative approach aims to enhance classification accuracy by leveraging a broader dataset. In figure 4.1 is an analysis of the trends observed in the classification accuracy as the training data expanded.

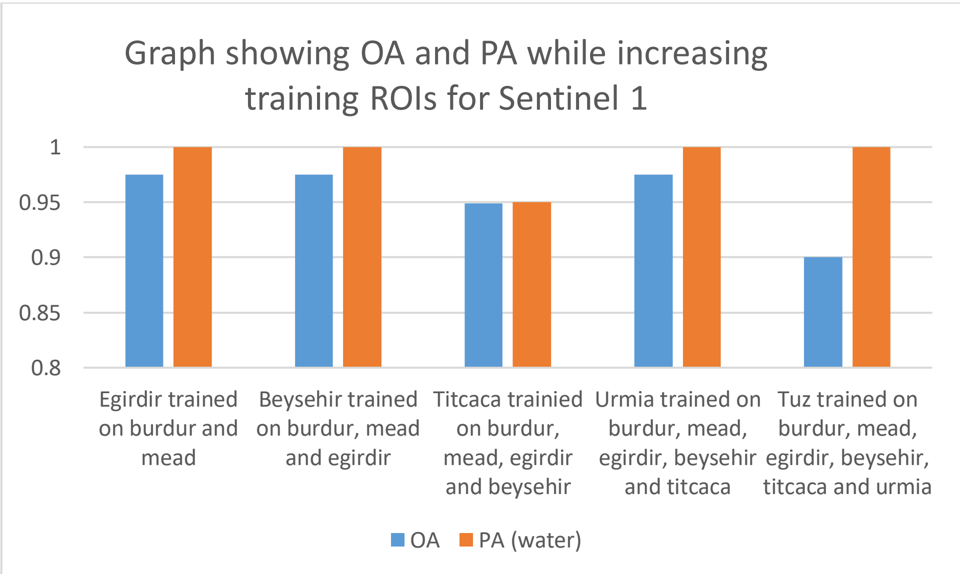

Figure 4.1. Graph of overall accuracy and producer's accuracy (water) while increasing training data for sentinel-1

The classification of Lake Egirdir, trained on the ROIs of Lake Burdur and Lake Mead, achieved near perfect accuracy (Figure 4.2a). This suggests that the training data from these lakes provided a highly representative dataset for the classification algorithm, allowing for precise delineation of water coverage in Lake Egirdir. Adding Lake Egirdir's ROI' GCPs to the training dataset for Lake Beysehir maintained this accuracy. This indicates that the inclusion of Egirdir's data did not introduce variability that could reduce accuracy. Instead, it likely provided additional representative samples that reinforced the algorithm's ability to classify water accurately.

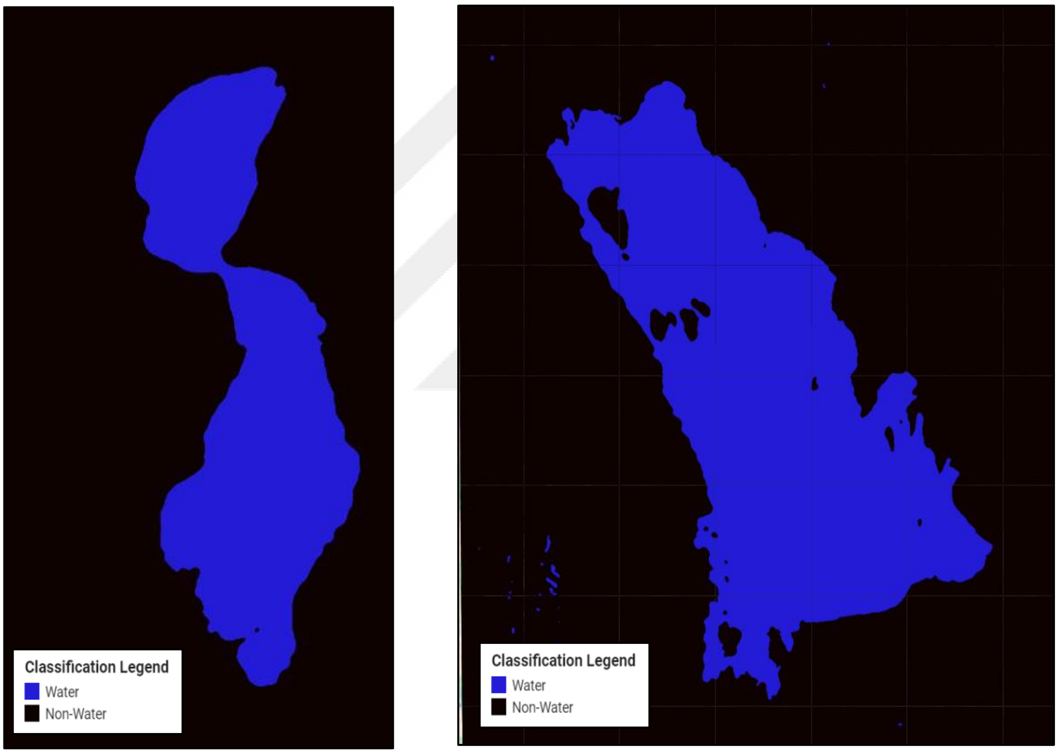

Figure 4.2. Sentinel-1 classification of Lake Egirdir (a) and Lake Beysehir (b) from 13/01/2023-25/02/2023

When Lake Titicaca was classified using an expanded training dataset that included GCPs from Burdur, Mead, Egirdir, and Beysehir, the accuracy slightly decreased. The OA dropped to 0.949, and PA for water was 0.95. This minor decline may be due to the increased complexity and diversity in the training data, as Lake Titicaca's environmental conditions differ more significantly from the other lakes. There is a clear misclassification of water in the central area of the lake where it is instead classified as non-water as can be seen in figure 4.3a, this area seems to be the main reason for the lower accuracy. For Lake Urmia in figure 4.3b, the addition of Lake Titicaca's data improved the classification accuracy, achieving an OA of 0.975 and perfect PA for water. This improvement suggests that the inclusion of diverse ROIs from a wide range of lakes helped the classification algorithm generalise better, especially for water bodies with varying characteristics.

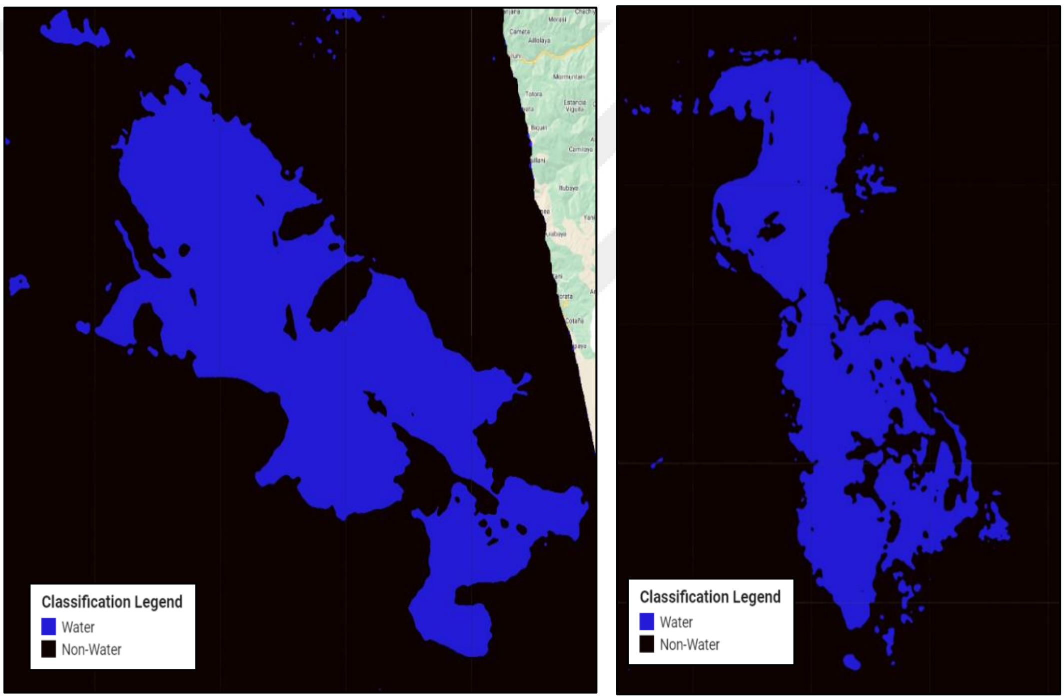

Figure 4.3. Sentinel-1 classification of Lake Titicaca (a) and Lake Urmia (b) from 13/01/2023-25/02/2023

Finally, the classification of Lake Tuz, which utilised the most extensive training dataset, resulted in an OA of 0.9 and perfect PA for water. The drop in OA compared to Urmia suggests that while the larger training set aids in water classification (as evidenced by the perfect PA), it may also introduce some complexity that affects overall classification accuracy.

Since Lake Urmia and Lake Tuz are both saline lakes with white backgrounds, adding lake Urmia to the training data for classifying Lake Tuz could have increased the accuracy of classification for Lake Tuz. Including data from a separate saline lake helps the model learn the unique spectral or backscatter characteristics associated with saline lakes. Furthermore, by incorporating data from Lake Urmia, the RF classifier is exposed to a broader range of variations in saline lake characteristics which can help the model become more reliable at distinguishing between saline lakes and other land cover types (Lary *et al.* 2016).

4.1.2 Sentinel-1 Classification Results of Lake Tuz using only Training Data from Lake Tuz

The accuracy of training and classifying a median filtered image of Lake Tuz using Sentinel-1 data between the dates of 13/01/23-25/02/23 is shown in table 4.1.

Table 4.1. Accuracies of Lake Tuz Sentinel-1 classification when only trained on Lake Tuz ROI

Overall Accuracy	Producer's Accuracy (water)
0.91	1

From these accuracies we can see that using Sentinel-1 data to both train and classify Lake Tuz shows very accurate results with an OA of 0.91. This compared to the accuracy of classifying Lake Tuz with an RFC trained on separate ROIs show similar results. This suggests that with Sentinel-1 data, the charactaristics detected by the satellite do not differ between locations and introducing more regions into the training data does not affect the classification process much.

Table 4.2. Importance of each variable when training the RFC on only Lake Tuz for classifying Lake Tuz using Sentinel-1 data

Variable	Importance Factor
VH	31.5
VV	30.78

These importance values show that the backscatter information captured by the VH polarization is slightly more informative for distinguishing the unique characteristics of Lake Tuz. VH polarization is generally more sensitive to variations in surface roughness and vegetation structure, however there was not a huge discrepancy between the two values, so both were important in building the classifier.

Figure 4.4. Sentinel-1 classified layer of Lake Tuz 13/01/2023-25/02/2023 using RFC trained only on Lake Tuz

4.1.3 Sentinel-1 Classification Results of Lake Tuz Throughout 2023

To begin this subsection, the importance of each variable used to train the RFC on Sentinel-1 data for classifying Lake Tuz will be discussed. Figure 4.3 shows the variable importance table.

Table 4.3. Importance of each variable when training the RFC for classifying Lake Tuz using Sentinel-1 data

Variable	Importance Factor
VV	31.82
VH	22.11

The variable importance table, derived from the random forest classifier trained on Sentinel-1 data, reveals that the VV polarisation played a more significant role in distinguishing between the different classes or features in the classification task compared to the VH polarisation. The higher importance of VV suggests that surface roughness characteristics were crucial for the classification, as VV polarisation is sensitive to these variations and is often more effective at discriminating between different land cover types, especially in areas with vegetation or varying surface textures. The lower importance of VH polarisation, which is more sensitive to moisture content, might indicate that moisture variations were not as critical in differentiating the classes of interest in this study.

However, as shown in table 4.2 in chapter 4.1.2, when training the RFC solely on Lake Tuz, VH polarization, capturing vegetation structure and subtle surface variations, takes precedence, implying its unique importance in identifying the lake's specific characteristics that did not apply to lakes globally.

Regarding the classification results of Lake Tuz (Figure 4.4) , the year began with a water coverage of 2170.01 km² at the beginning of January, which then increased to 2333.82 km² by the second 12-day period. However, a significant drop to 1955.02 km² was observed in the subsequent period, followed by a further decrease to 1921.96 km² in early February. Notably, there was a remarkable increase to 2666.57 km² by the end of February, marking the highest water coverage recorded for the year. This period of fluctuation indicates a dynamic hydrological environment influenced by seasonal factors such as varying precipitation and evaporation levels.

In March, the water coverage saw a reduction to 2037.04 km², followed by an increase to 2369.69 km². This period highlights the lake's response to seasonal changes, possibly due to melting snow or rainfall. The coverage then decreased steadily through April and May, reaching 1810.07 km² by mid-May. This trend suggests a gradual decline, likely influenced by increasing temperatures and evaporation rates as spring progressed into early summer.

The summer months saw substantial decreases in water coverage, starting from 1871.85 km² in early June to a significant low of 1200.81 km² by mid-July. The lake's extent slightly recovered to 1349.14 km² but continued to fluctuate, reaching 1162.28 km² by late August. These reductions are typical of arid regions during summer, where high evaporation rates and reduced inflow contribute to shrinking water bodies.

Entering October, the lake began to recover, with water coverage increasing to 2173.2 km². This recovery continued into November, maintaining levels above 2000 km², with a peak of 2063.87 km² in late October. By December, the coverage was stable around 1800 km², ending the year at 2029.08 km². This period likely reflects increased precipitation and reduced evaporation as cooler temperatures set in, contributing to the replenishment of the lake.

This can all be seen in figure 4.5.

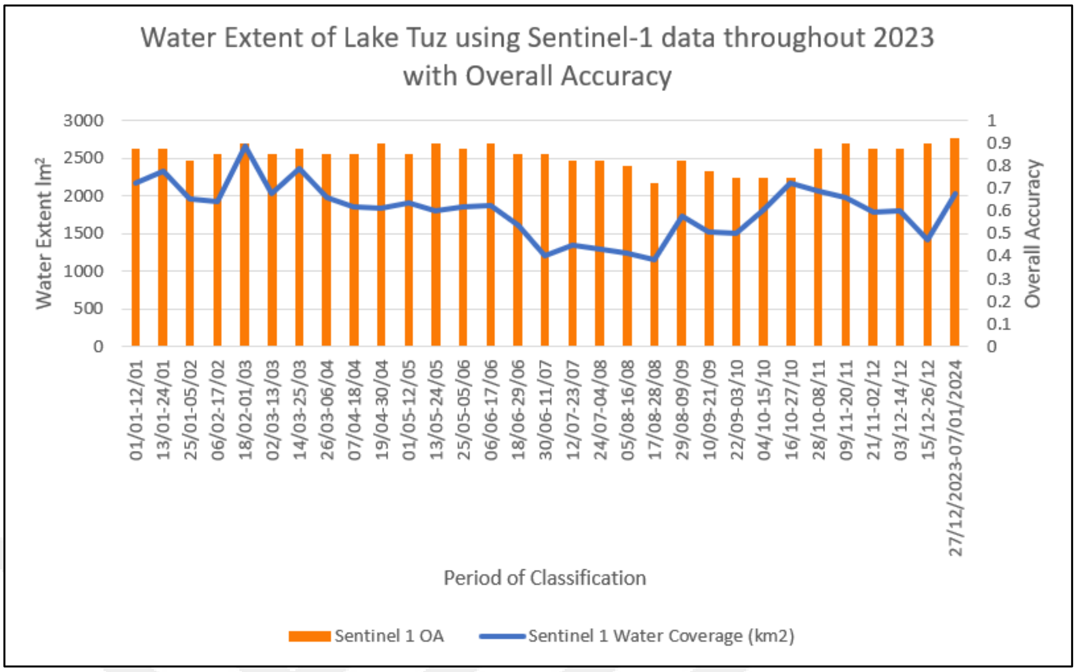

Figure 4.5. Graph of sentinel-1 and overall accuracy and water extent in km^2 within the Lake Tuz ROI

The overall accuracy (OA) of the image classification techniques used for these measurements ranged from 0.725 to 0.925, indicating a high degree of confidence in the data. Periods with lower accuracy (e.g., 0.725 in late August) may correspond to challenging conditions for satellite imaging, such as SAR being sensitive to surface roughness. Variations in the lakebed's texture can affect backscatter signal, leading to misclassification.

Through visual comparison with a plain Sentinel-2 image of the same dates, there appears to be possible misclassification in the south eastern portion of the lake possibly due to the smoothness of this area caused by frequent flooding and left-over moist soil. In figure 4.6 is an image of Lake Tuz taken from Sentinel-2.

Figure 4.6. Sentinel-2 image of Lake Tuz from 13/01/2023-25/02/2023 with moist soil area shown in red square

In figure 4.7 we can see an image of classified sentinel-1 data of the same dates for visual comparison with the sentinel-2 image.

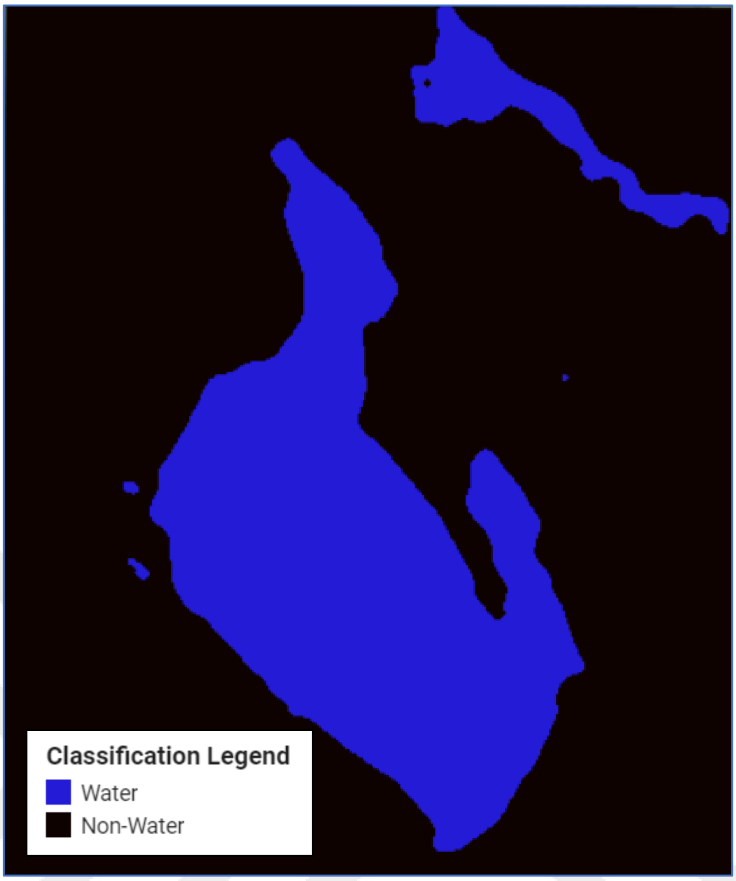

Figure 4.7. Sentinel-1 classified layer of Lake Tuz 13/01/2023-25/02/2023

The southern part of the lake is generally made up of not water nor salt but large quantities of moist soil with seasonal floods also occurring in this area (Bilgilioğlu et al. 2021). The classification result of sentinel-1 southern areas could be due to areas of moist soil causing low backscatter values, causing it to be classified as water. It is important to note however that for the accuracy assessment of these dates, there was uncertainty around whether or not to mark this area as being water with validation GCPs due to its high moisture content and also due to the fact that it was classified as water in Dynamic World. Ultimately, between the dates of 13/01 to 25/02, it was marked as non-water by validation GCPs despite the possibility of flooding, meaning that this area was classified incorrectly. Throughout the rest of the year however, the validation GCPs were changed, while this area was mostly marked as non-water, occasionally parts of it were marked as water.

This area being classified as water has meant that more area has been classified as water than what should have been, leading to an incorrect increased extent of water area according to Sentinel-1 classification, likely due to SAR's sensitivity to moisture. This is reflected by the comparison between the OA and the PA (water) of Lake Tuz. Where all water validation GCPs were placed on areas eventually classified as water, some non-water validation GCPs were placed on areas that were also classified as water. This means that the PA for non-water is lower than the PA (water) and brings down the OA.

A visual comparion can be drawn between this and the classified image of Lake Tuz when the RFC was trained only on lake Tuz. As shown in figure 4.4 of chapter 4.1.2, both classified images are extremely similar, with overclassification of the moist soil area in the south portion of the lake.

4.2 Sentinel-2 Results

4.2.1 Increasing Sentinel-2 Training Data

The graph in figure 4.8 presents the overall accuracy (OA) and producer's accuracy (PA) of water for the image classification of multiple lakes, utilising Sentinel-2 imagery. As with the sentinel-1 data, the lakes analysed include Egirdir, Beysehir, Titicaca, Urmia, and Tuz, with each successive lake classification incorporating ROIs from previously classified lakes into its training data.

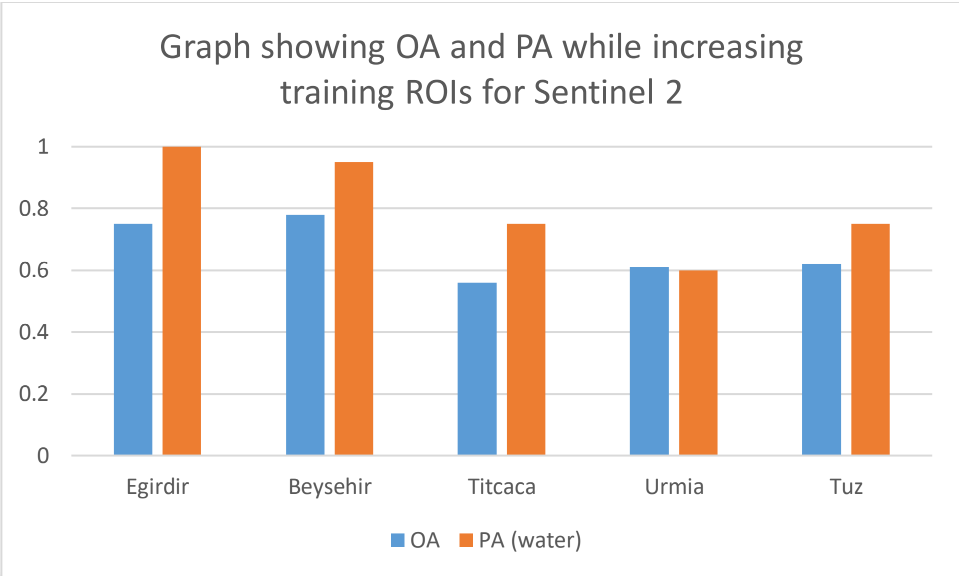

Figure 4.8. Graph showing overall accuracy and producer's accuracy (water) while increasing training data for Sentinel-2

The classification of Lake Egirdir, trained on the ROIs of Lake Burdur and Lake Mead, achieved a reasonably high OA of 0.75 and perfect PA for water. This suggests that the training data from these lakes provided a sufficiently representative dataset for the classification algorithm, allowing for precise delineation of water coverage in Lake Egirdir. Adding Lake Egirdir's ROI to the training dataset for Lake Beysehir improved the OA to 0.78 and resulted in a slightly lower PA for water of 0.95. This indicates that while the inclusion of Egirdir's data helped improve the overall accuracy, there may have been some variability introduced that affected the water classification slightly.

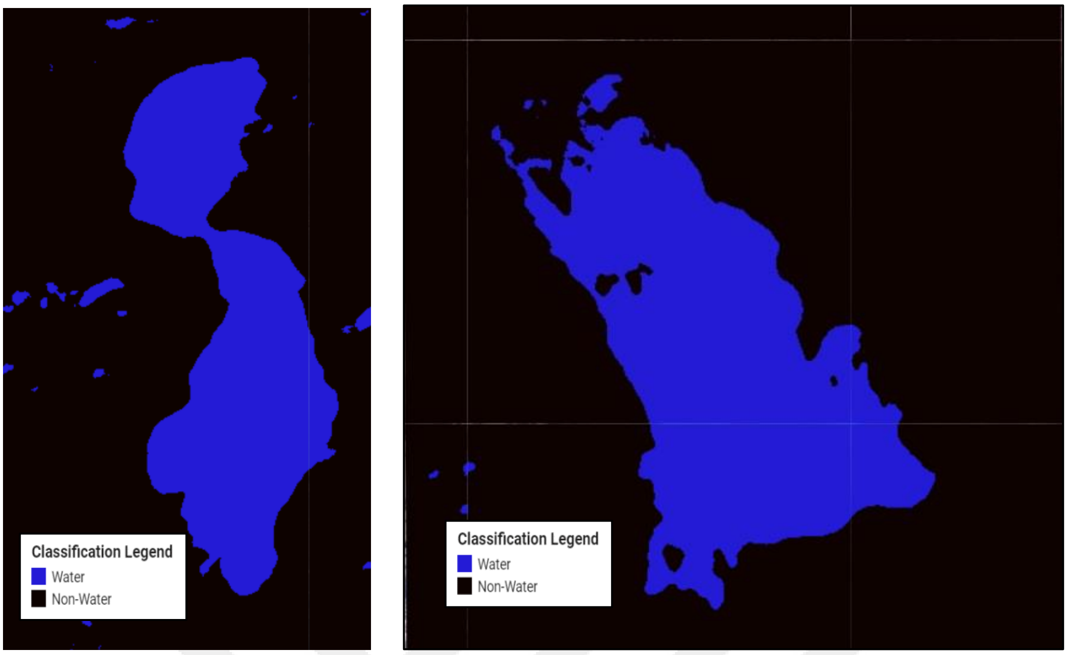

Figure 4.9. Sentinel-2 classification of Lake Egirdir (a) and Lake Beysehir (b) from 13/01/2023-25/02/2023

When Lake Titicaca was classified using an expanded training dataset that included ROIs from Burdur, Mead, Egirdir, and Beysehir, the accuracy decreased significantly. The OA dropped to 0.56, and PA for water was 0.75. This decline may again be due to the increased complexity and diversity in the training data, as Lake Titicaca's environmental conditions differ more significantly from the other lakes, affecting the RFC's performance. For Lake Urmia, the inclusion of Lake Titicaca's data resulted in an OA of 0.61 and a PA for water of 0.6. While there is a slight improvement in overall accuracy compared to Titicaca, the water classification accuracy remains relatively low. This suggests that the diverse training set helped the algorithm generalise better, but the variability introduced by Titicaca's conditions still posed challenges.

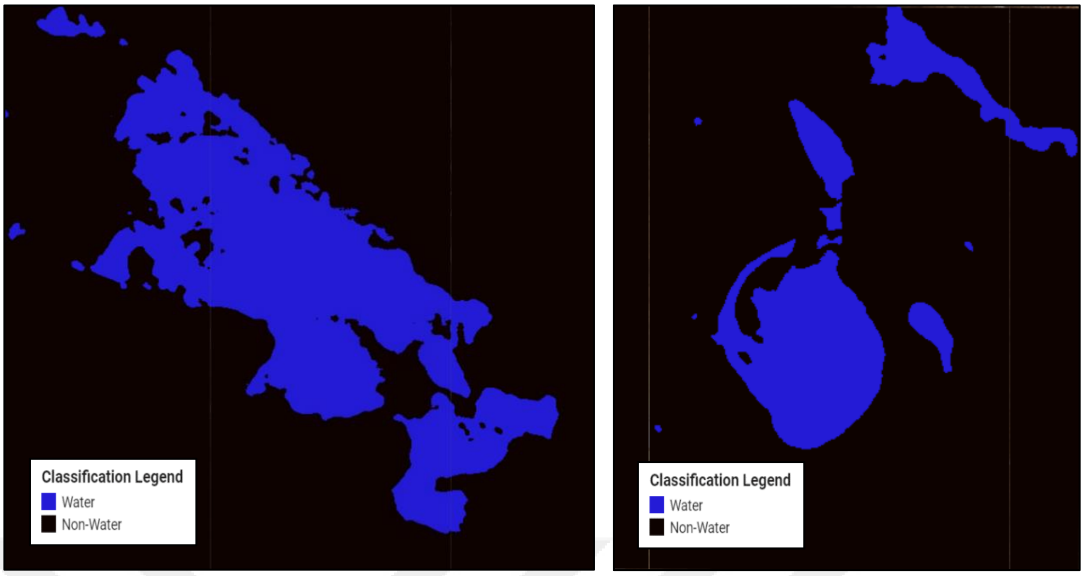

Figure 4.10. Sentinel-2 classification of Lake Titicaca (a) and Lake Tuz (b) from 13/01/2023-25/02/2023

Finally, the classification of Lake Tuz, which utilised the most extensive training dataset, resulted in an OA of 0.62 and a PA for water of 0.75. The slight improvement of the OA here compared to that of the classification of Lake Urmia indicates that the larger training set aids in overall classification. However, the PA for water suggests that the variability introduced by the diverse training data still affects the accuracy of water classification. Furthermore, the low PA (water) compared to that of Sentinel-1, shows that many areas of water were being classified as a non-water class. By examining figure 4.10 (b) we can see portions of the lake being classified mostly as vegetation but also with some urban and some snow.

4.2.2 Sentinel-2 Classification Results of Lake Tuz using only Training Data from Lake Tuz

The accuracy of training and classifying a median filtered image of Lake Tuz using Sentinel-2 data between the dates of 13/01/23-25/02/23 is shown in table 4.4.

Table 4.4. Accuracies of Lake Tuz Sentinel-2 classification when only trained on Lake Tuz ROI

Overall Accuracy	Producer's Accuracy (water)
0.73	0.89

Here we can see notably higher accuracy results when training the RFC on only Lake Tuz compared to when training the RFC on global lakes. Both OA and PA (water) are found to be much higher when classifying lake Tuz using a model trained only on lake Tuz. This strongly hints that Sentinel-2 data captures features that are highly specific to Lake Tuz's local environment. These features might be related to its unique spectral reflectance properties, influenced by factors like water quality, mineral content, or surrounding vegetation. The global model, trained on a diverse set of lakes, may not have encountered these specific features frequently enough to learn to recognize them reliably. Table 4.5 shows importance rankings of the bands.

Table 4.5. Importance of each variable when training the RFC on only Lake Tuz for classifying Lake Tuz using Sentinel-2 data

Band	Importance Factor
NDBI	18.44
B1	17.2
B11	16.92
NDVI	15.68
NDWI	15.54
B3	13.31
B6	13.02
B4	12.44
B5	11.61
B8A	10.11
B7	10.11
B2	9.44

The high value of NDBI highlights the significance of built-up areas near the lake. The importance of B1 (Coastal Aerosol) shows influence of atmospheric conditions and aerosols, potentially due to the lake's proximity to the coast. B11 (Shortwave Infrared), sensitive to vegetation and soil moisture, along with NDVI and NDWI, highlights the important role of land cover and hydrological conditions in characterizing the lake. Additionally, the importance of B3 (Green) and B4 (Red) highlights the contribution of vegetation health and density to the classification.

In figure 4.11 we can see that when training the RFC on only Lake Tuz, classification of water becomes more accurate in comparison to the classification shown in figure 4.10 (b) in chapter 4.2.1. In figure 4.11 we can see that many parts of the north west of the lake that was classified incorrectly using the globally trained RFC, have been classified correctly using the Lake Tuz trained RFC. This is further backed up by the higher accuracy results using the Lake Tuz trained RFC as shown in table 4.4.

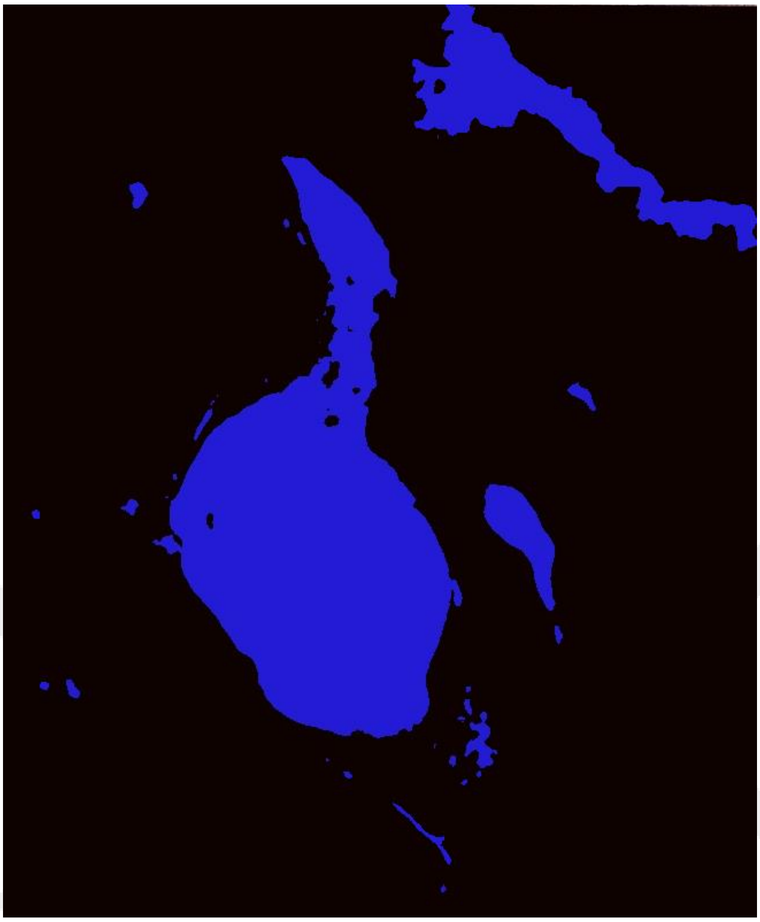

Figure 4.11. Sentinel-2 classified layer of Lake Tuz 13/01/2023-25/02/2023 using only RFC trained on Lake Tuz

4.2.3 Sentinel-2 Classification Results of Lake Tuz Throughout 2023

To begin this subsection, the importance of each variable used to train the RFC on Sentinel-2 data for classifying Lake Tuz will be discussed, as seen in table 4.6.

Table 4.6. Importance of each variable when training the RFC for classifying Lake Tuz using Sentinel-2 data

Variable	Importance Factor
NDBI	75.93
B11	75.22
B8	72.69
NDVI	72.21
B6	69.47
B1	67.31
B2	67.02
NDWI	66.94
B7	63.7
B8A	63.59
B3	57.91
B5	57.37
B4	53.72

The variable importance table, derived from the Random Forest classifier trained on Sentinel-2 data, reveals that B11 (Short Wave Infrared) and NDBI (Normalised Difference Built-up Index) were the most influential variables in distinguishing between different land cover classes. The prominence of these variables suggests that built-up areas or bare soil played a significant role in the classification process. The importance of the other spectral indices, NDVI and NDWI, shows that they supplied a high level of effectiveness in capturing distinct land cover characteristics. The relatively high importance of near-infrared bands (B8, B8A, B5) indicates the relevance of vegetation health and biomass in the classification. While less influential than other bands, the visible bands (B1, B2, B3, B4) still contribute to the classification by providing information about soil and surface properties.

It should be noted that when comparing these importance values to the values of the the RFC trainined only on Lake Tuz as can be seen in table 4.5 in chapter 4.2.2, NDBI remains a top predictor in both models. In addition, the global model emphasizes B11 (Shortwave Infrared) and B8 (Near Infrared), suggesting a greater focus on vegetation and moisture content for distinguishing lakes on a broader scale. Notably, NDWI's importance diminishes in the global model, indicating that while water is crucial, other factors like vegetation and built-up areas become more distinguishing globally. Additionally, the reduced role of B1 (Coastal Aerosol) in the global model suggests that atmospheric conditions are less universally critical for lake classification.

Moving on to the classification results, the year began with a relatively low water coverage of 685.86 km² during the first 12-day period in January. This quickly rose to 886.84 km² in the second period and further to 1042.3 km² by early February. These increases suggest initial water inflow, possibly from precipitation or upstream sources. Despite a slight decrease to 1012.17 km² in mid-February, the coverage remained above 1000 km² through early March. This period shows a generally increasing trend, with the lake responding to seasonal changes and potentially higher water inputs.

The water coverage peaked at 1185.44 km² in mid-March, followed by a slight reduction to 1158.28 km². The trend of minor fluctuations continued, with water coverage remaining around 1100 km² through April, ending at 1112.69 km². However, during May there was a noticeable decline, dropping to 942.95 km². This gradual decrease likely reflects increasing temperatures and evaporation as spring transitions into summer, coupled with potentially reduced inflows.

Summer months marked a sharp decline in water coverage, from 917.7 km² in mid-June to 698.16 km² by early July. The decrease continued, reaching a low of 245.29 km² by late August. These reductions are indicative of high evaporation rates typical in arid regions during summer, along with possible water extraction for agricultural or other uses. This period represents the lowest water coverage recorded throughout the year.

Coming into October, the lake began to recover, with water coverage increasing to 452.33 km² and further to 849.24 km² by late November. This recovery trend continued into December, reaching 1187.17 km², and ending the year at 1109.21 km². This resurgence is likely due to seasonal precipitation and reduced evaporation rates as temperatures cool.

All this data can be seen in the graph of figure 4.12.

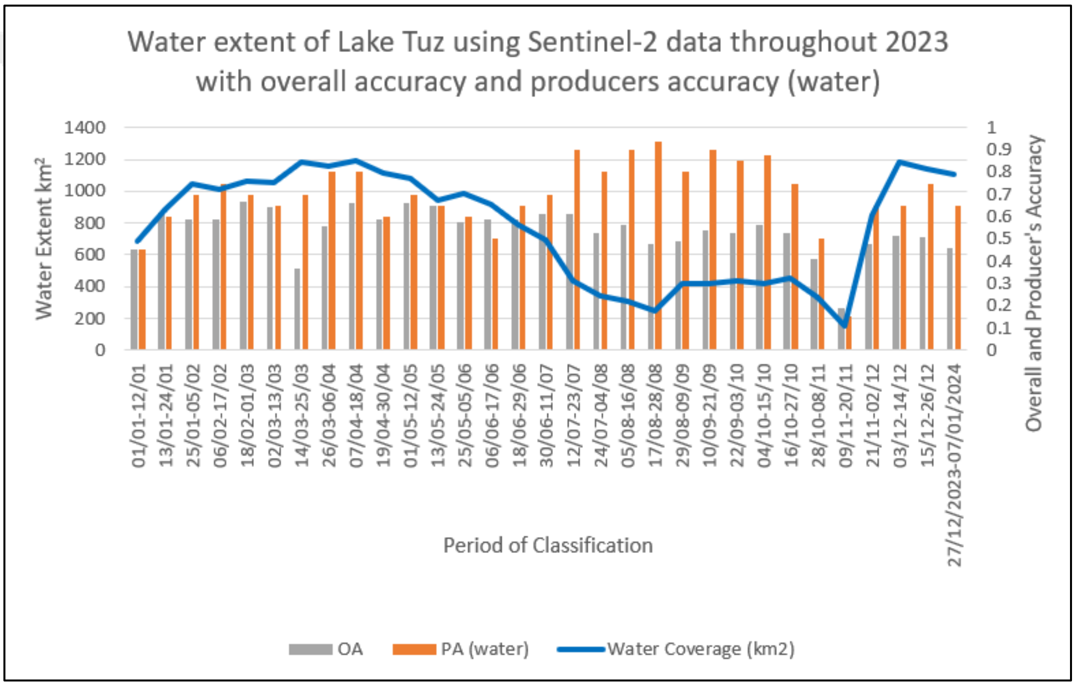

Figure 4.12. Graph of sentinel-2 and overall accuracy and water extent in km^2 within the Lake Tuz ROI

The OA values in this dataset range from 0.19 to 0.67, with the highest accuracy recorded in late February (0.67) and the lowest in mid-November (0.19). These variations indicate periods of higher classification reliability interspersed with more challenging periods for accurate measurement. The PA for water ranges from 0.15 to 0.9375, with the highest accuracy recorded in mid-August (0.9375) and the lowest in late November (0.15). The PA values generally show better performance, particularly in periods of significant water coverage. The low accuracy between the dates 09/11-20/11 will be due to the data having cloud coverage increased to 80 at this time. The RGB image from Sentinel-2 of this time period can be seen in figure 4.13 showing extensive cloud cover and obscured ground features.

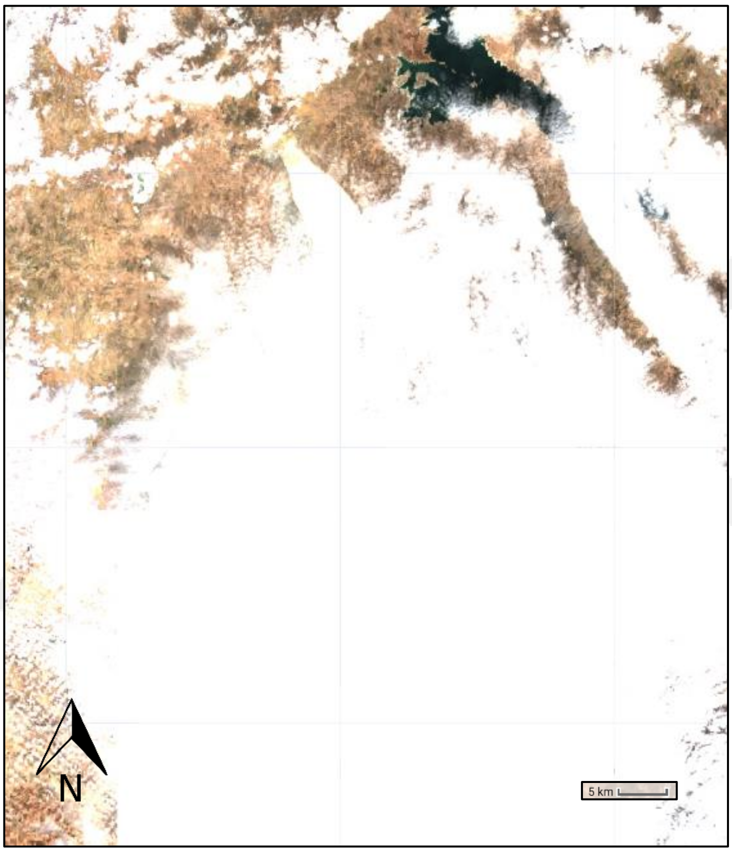

Figure 4.13. RGB image taken from Sentinel-2 of Lake Tuz between the dates 09/11/2023-20/11/2023

Lack of the snow class during the summer may have improved Sentinel-2 classification as salt/salt water was being confused as snow during the winter months. This could be seen during the training process while classifying Lake Urmia as can be seen in figure 4.14.

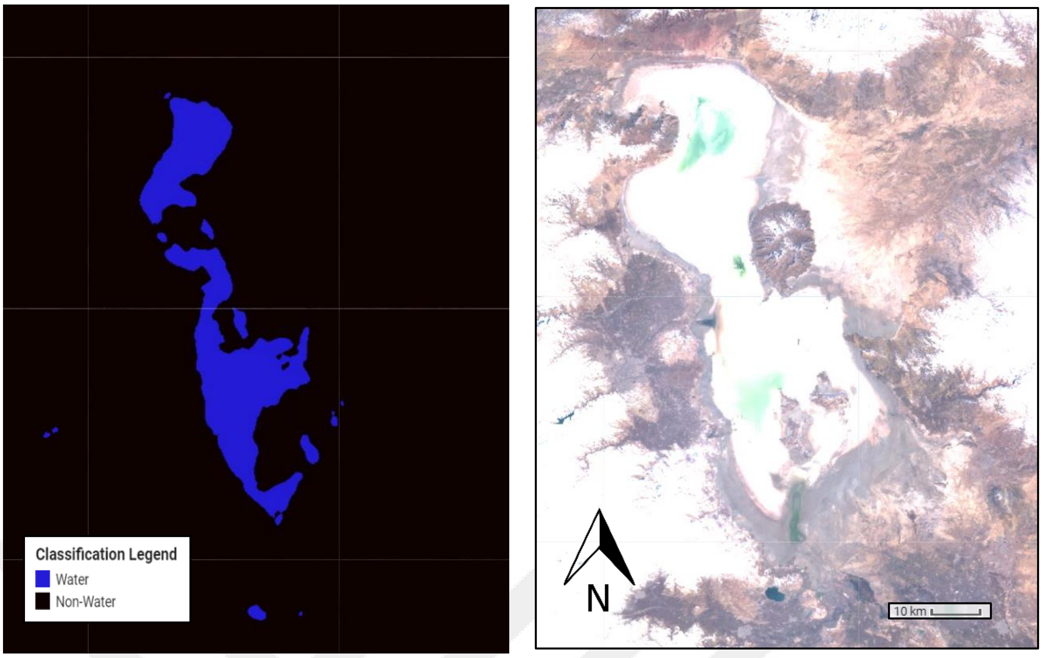

Figure 4.14. Classified Sentinel-2 median image (a) and Sentinel-2 median RGB image (b) of Lake Urmia from 13/01/23-25/02/23

As seen in figure 4.14 by visual inspection, lots of the water/salt deposit areas, particularly on the edges of the lake, are classified as non-water.

Furthermore, there were multiple occasions where cloud cover was also confused with the non-water classes during the winter months. This could be seen during the periods where the cloud coverage limit had to be increased due to an otherwise lack of data. The RGB image of Lake Tuz with high cloud cover can be seen in figure 4.15 (b) of Lake Tuz below. The corresponding classification result can be seen in figure 4.15 (a) which shows much of the clouds in the image being classified as snow.

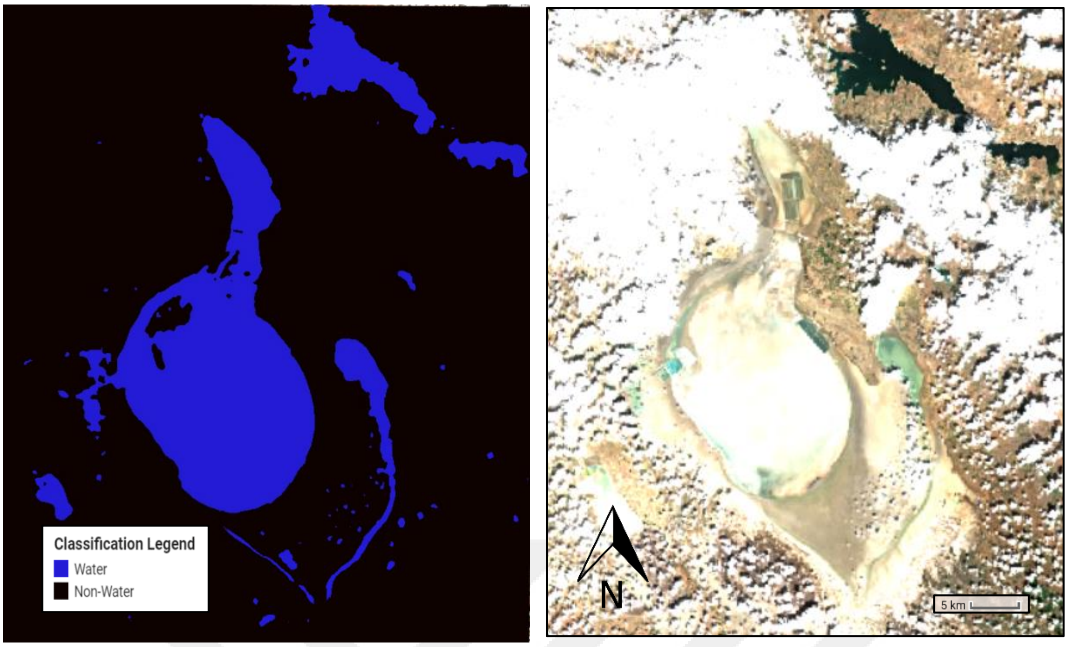

Figure 4.15. Classified Sentinel-2 median image (a) and Sentinel-2 median RGB image (b) of Lake Tuz from 14/03/23-25/03/23

It is worth noting that in figure 4.15, the RGB image does not clearly show water within the area of the lake, yet the classification image does. This could be due to shallow depth and high salinity of the lake (Dengiz et al. 2010). The shallow depth could cause the salt to appear more clearly through the water in the RGB image. This means the RGB image does not seem to be sensitive enough to detect shallow water bodies, especially if they are highly saline. The classification algorithm, on the other hand, is specifically designed to identify water bodies based on spectral signatures, even if they are shallow or have high salinity.

Another example of cloud cover causing low accuracy can be seen during the dates 09/11/23-20/11/23 as mentioned earlier. This was one of the dates wherein which the cloud cover limit had to be increased due to a lack of less cloudy data, and subsequently had the lowest accuracy out of all the data, with an overall accuracy of 0.19. The classification layer for these dates can be seen in figure 4.16 showing the cloud cover causing lots of the ROI to be classified as Non-Water.

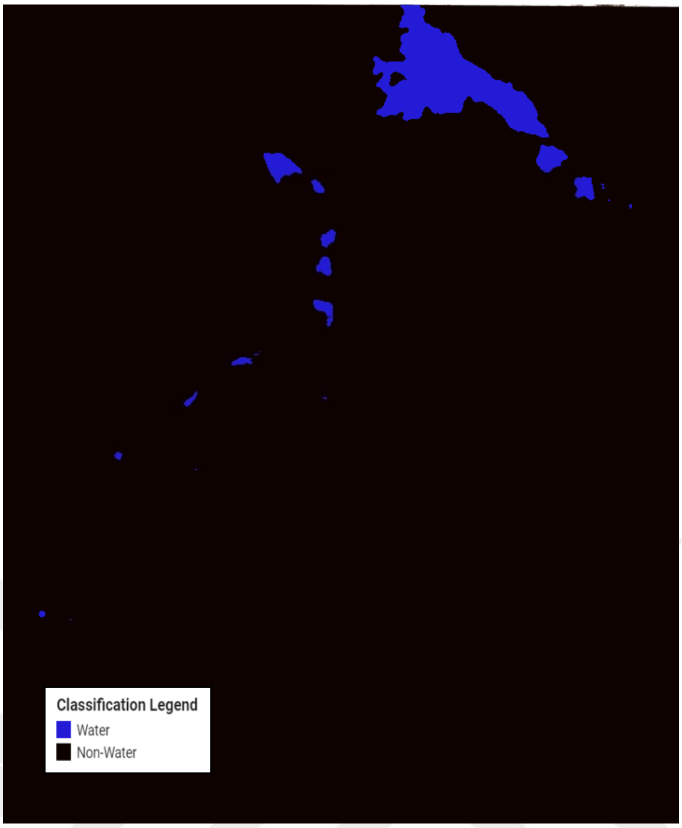

Figure 4.16. Classified Sentinel-2 median image of Lake Tuz from 09/11/23-20/11/23

The summer to autumn months did however seem to improve the Sentinel-2 producer's accuracy of water, possibly due to less cloud cover interfering with the images. This trend of improved accuracy can be seen occurring from 30/06/23 to 15/10/23.

On the subject of non-water classification, Sentinel-2 was especially ineffective at classifying non-water classes as can be surmised from the higher producer's accuracy of water compared to the lower overall accuracy. There was a frequently high level of confusion between the 'vegetation', 'built', 'bare' and 'snow' classes. Below are tables 4.7, 4.8 and 4.9, 3 confusion matrices of the classes taken from equally spaced-out dates in 2023.

Table 4.7 Confusion matrix of Sentinel-2 image from dates 01/01/2023-12/01/2023

	Water	**Built**	**Vegetation**	**Bare**	**Snow**
Water	11	3	2	3	1
Built	0	10	1	9	0
Vegetation	1	3	12	4	0
Bare	0	7	0	13	0
Snow	1	3	0	16	0

In January, the Water class had 11 correct classifications but was often confused with Built, Bare, and Vegetation, suggesting spectral similarities in these areas. The Built class also faced challenges, frequently being misclassified as Bare, indicating that the spectral properties of these two classes are closely related, especially in transitional or urban fringe areas. The Vegetation class, while correctly identified in 12 instances, saw some misclassification with Built and Bare classes. This points to the complexity of accurately identifying vegetation in mixed or sparse regions. The bare class had a significant number of correct identifications but was commonly mistaken for built, further emphasising the spectral overlap issue. The Snow class was the most problematic, with no correct classifications and frequent confusion with Bare land.

Table 4.8 Confusion matrix of Sentinel-2 image from dates 18/06/2023-29/06/2023

	Water	**Built**	**Vegetation**	**Bare**
Water	15	1	4	0
Built	0	8	7	5
Vegetation	1	9	8	2
Bare	1	4	1	14

During another classification in June, water was accurately classified in 15 instances, with minimal confusion, being misclassified only once as built and four times as vegetation. This indicates a strong performance in identifying water bodies, though some overlap with vegetation suggests areas where water and vegetative cover may be intermixed. The built class shows significant misclassification, with only eight correct instances. It was often confused with vegetation and bare, showing difficulties in distinguishing built-up areas from vegetation or bare classes. Vegetation classification accuracy was similarly compromised, with only eight correct identifications and frequent misclassification as built along with some overlap with water and bare. This again points to spectral similarities and mixed pixels in regions where vegetation and built structures coexist.

Table 4.9 Confusion matrix of Sentinel-2 image from dates 15/12/2023-26/12/2023

	Water	**Built**	**Vegetation**	**Bare**	**Snow**
Water	15	1	1	3	0
Built	0	12	7	1	0
Vegetation	0	12	5	3	0
Bare	1	5	5	8	1
Snow	3	1	1	7	8

In December, water was accurately classified 15 times but showed some confusion with bare, suggesting more spectral similarities due to sparse vegetation or muddy banks. built and vegetation classes faced significant misclassification, with built often mistaken for vegetation and vice versa. This indicates again some overlapping spectral characteristics in urban or semi-urban areas where these classes coexist. Bare land obtained moderate accuracy but was frequently confused with built, vegetation, and snow. Snow classification showed considerable misclassification, particularly with bare, as was also the case in January.

It is interesting to note that vegetation was calculated to have much larger cover in the spring and early summer months as compared to the winter. Between the dates of 18/06/2023-29/06/2023, vegetation was calculated to be at a coverage of 2312.69 km squared, in contrast to 01/01/2023-12/01/2023 where vegetation was at 607.3 km squared and 15/12/2023-26/12/2023 where vegetation was at 1687.22 km^2. This can be seen in the graph of calculated coverage of each class in the Figure 4.17.

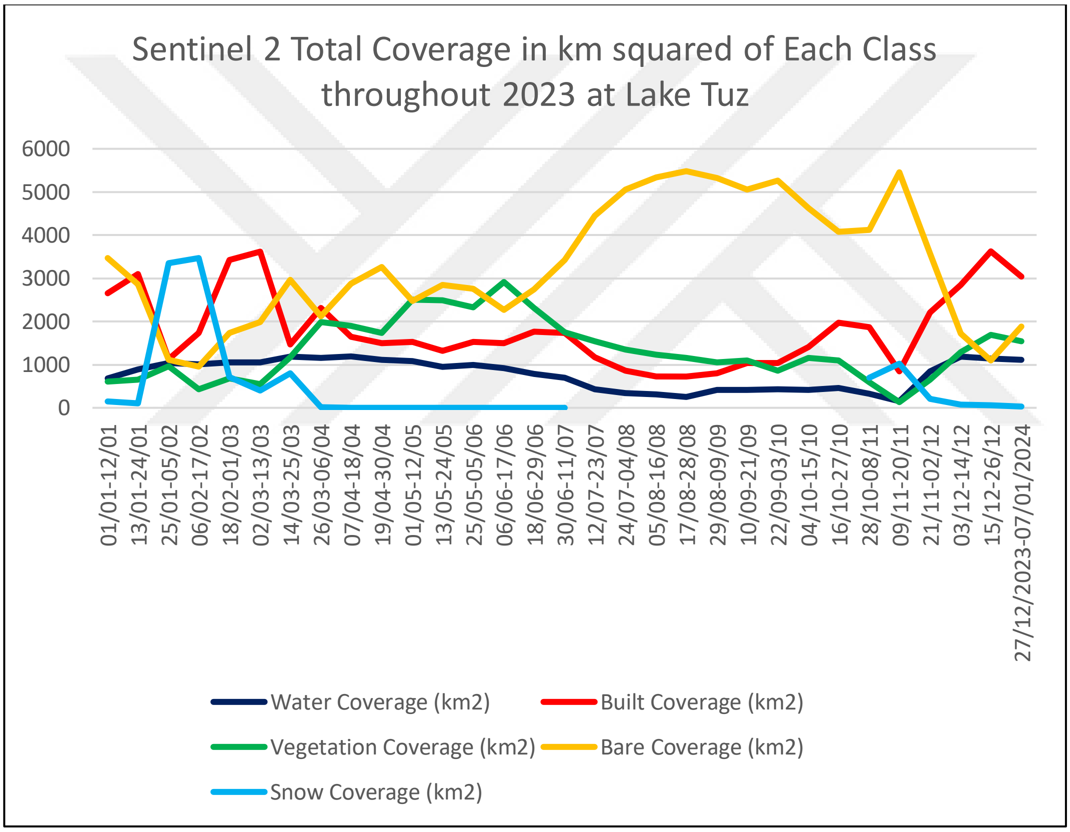

Figure 4.17. Sentinel-2 extent of all classes within the area of the Lake Tuz ROI throughout 2023

This increase in vegetation during the spring months is to be expected, however it could also be the reason for increased confusion of the vegetation class due to increased diversity in plant growth. This increased complexity can introduce a variety of spectral signatures, making it challenging for the classification algorithm to accurately distinguish between vegetation and other classes (Manandhar *et al.* 2009). The later decrease in vegetation cover could indicate less complexity in the spectral signatures due to less diversity, resulting in the improved classification of vegetation during 15/12/2023-26/12/2023. There is also a clear increase in bare land cover during the late summer and autumn months which coincided with a slight decrease in water coverage as well, indicating bare land emerging as the water levels decrease. This trend however is not shown to be highly correlated as the increase of bare land extent is much higher than that of the decrease of water extent. Urban extent is shown to be highly varying which emphasises unreliability in the classification, as urban is expected to change very little throughout the year due to its more permanent nature.

4.3 Comparison of Sentinel-1 and Sentinel-2

4.3.1 Comparison of Calculated Water Extent

Throughout 2023, the water extent of Lake Tuz exhibited significant fluctuations based on data from Sentinel-1 and Sentinel-2 imagery as shown in figure 4.18.

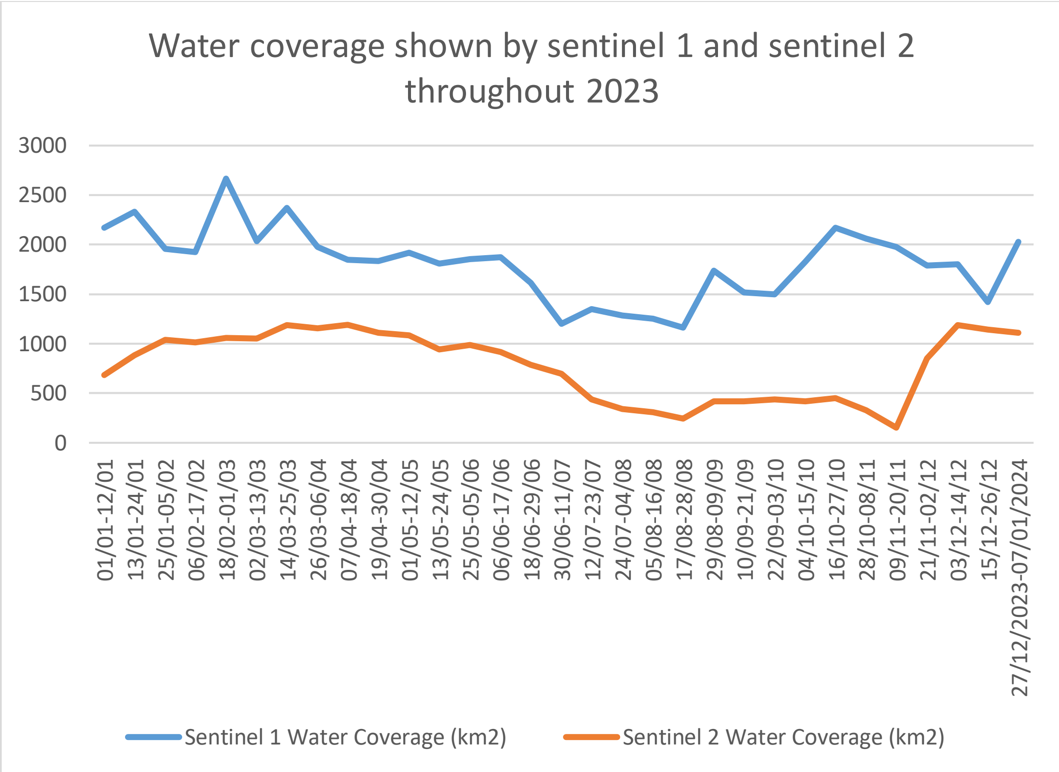

Figure 4.18. Comparison of water coverage for Sentinel-1 and Sentinel-2 data

According to Sentinel-1 data as seen in figure 4.18, the year began with a water extent of 2170.01 km² in early January, which peaked at 2333.82 km² by mid-January. A decline followed, dropping to 1921.96 km² by mid-February, before a significant increase in late February to 2666.57 km², marking the highest value of the year. From early March to mid-April, water extent fluctuated, peaking at 2369.69 km² in mid-March and declining to 1834.35 km² by the end of April. Stability was observed from May to June, with values ranging between 1810.07 km² and 1871.85 km². However, a notable decrease occurred in early July to 1200.81 km², followed by fluctuations through July and August, peaking at 1349.14 km² and then declining to 1162.28 km². A significant increase in early September to 1736.04 km² was noted, followed by a decrease to 1499.47 km² by late September. From October to early November, the water extent remained fairly consistent around 1500 km². A rise in late November to early December brought the extent to 1977.12 km², ending the year at 2029.08 km² in early January 2024.

Sentinel-2 data reflected similar trends with some differences in magnitude. The water extent began at 685.86 km² in early January and increased to 886.84 km² by mid-January, continuing to peak at 1042.3 km² in late January, and remaining above 1000 km² until mid-February. A slight decline by early March was followed by another peak of 1185.44 km² in mid-March. From late March to early June, the extent stabilised between 1158.28 km² and 1112.69 km². A significant decrease in mid-June saw values drop to 698.16 km². Through July and August, the extent continued to decline, reaching its lowest value of 245.29 km² in late August. However, a notable increase in early September to 418.98 km² stabilised around 400 km² until late October. Early November recorded a significant drop to 152.73 km², followed by a peak in early December to 1187.17 km², ending the year at 1109.21 km² in early January 2024.

Overall, both datasets show varying water extent variations for the Lake Tuz ROI throughout 2023, with both data sets showing the same peaks and declines at similar times of the year, corresponding to seasonal changes. However, Sentinel-1 data showed a much higher water coverage compared to Sentinel-2 data. One minor reason for the discrepancy of water extent between both data sets could be cloud cover obscuring water during certain 12-day periods causing misclassification. This high level of cloud cover however does not apply throughout the whole year and therefore is not the main reason for the discrepancy in water extent between Sentinel-1 and Sentinel-2. As discussed previously in chapter 4.1.2, this difference could largely be due to the sensitivity of sentinel-1 regarding the detection of moisture in soil and other surrounding areas of the lake. Moreover, the surface of Lake Tuz can vary in roughness due to salt crusts and water levels. SAR is sensitive to surface roughness, which makes it more effective at detecting water bodies with varying textures and salinity levels. Optical sensors might struggle to distinguish between wet salt flats and actual water bodies. The presence of vegetation and algal blooms in and around Lake Tuz can also affect the reflectance properties detected by

Sentinel-2. Algal blooms, for instance, can alter the spectral signature of the water, making it harder for optical sensors to accurately classify the water extent (Keith 2020). This optical complexity of the water could have made its classification more difficult.

A study by Ceyhan (2016) studied lake Tuz from 2000 to 2015, the water extent of the lake was shown to be vary throughout each year drastically. In this study, the water extent of Lake Tuz in 2015 is shown to sit at 805 km^2 in June, 696 km^2 in July, 401 km^2 in August and 214 km^2 in September. The study by Ceyhan (2016) only included measuring the basin of the lake whereas the ROI of lake Tuz used in this thesis also contains the Kızılırmak River north of Lake Tuz. This increased the total calculated water extent of the lake Tuz ROI for Sentinel-1 and Sentinel-2 data comapred to the 2016 study. Comparisons can still be drawn from this however, with the 2016 study showing closer values to the Sentinel 2 data as far as water extent is concerned.

4.3.2 Comparison of Accuracies

Here we have classified Sentinel-1 and Sentinel-2 images of Lake Tuz taken from equally spaced-out dates throughout 2023. The dates from which these classification layers were taken are the same as those used to obtain the confusion matrices in chapter 4.2.2. The corresponding Sentinel-2 images are seen in figure 4.20 along with the succeeding Sentinel-1 images in figure 4.21 for direct comparison. The rest of the classified images throughout the whole year are present in the appendices. Reclassified dynamic world images are also shown for comparison in figure 4.19.

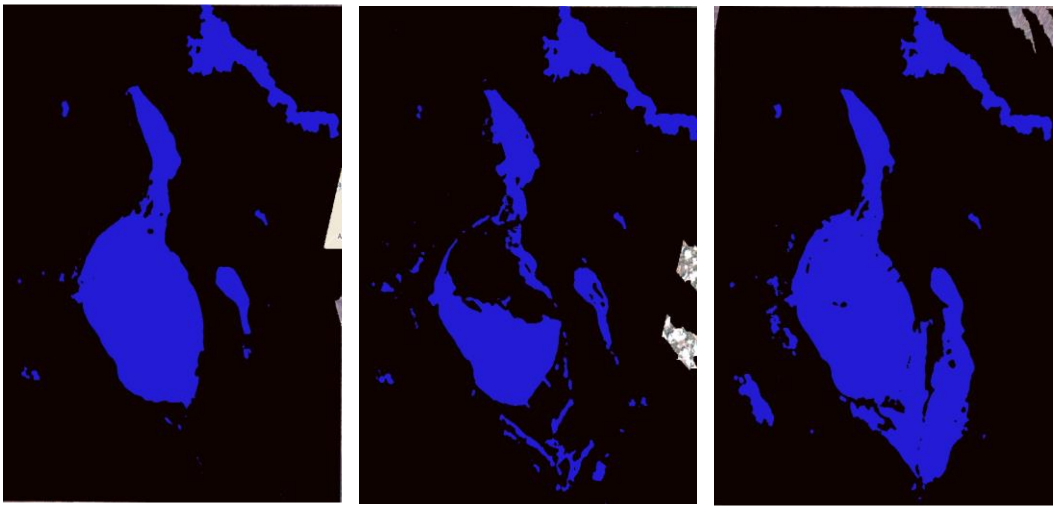

Figure 4.19 Re-classified Dynamic World images from 01/01/2023-12/01/2023 (a) to 18/06/2023-29/06/2023 (b) to 03/12/2023-15/12/2023 (c) in order

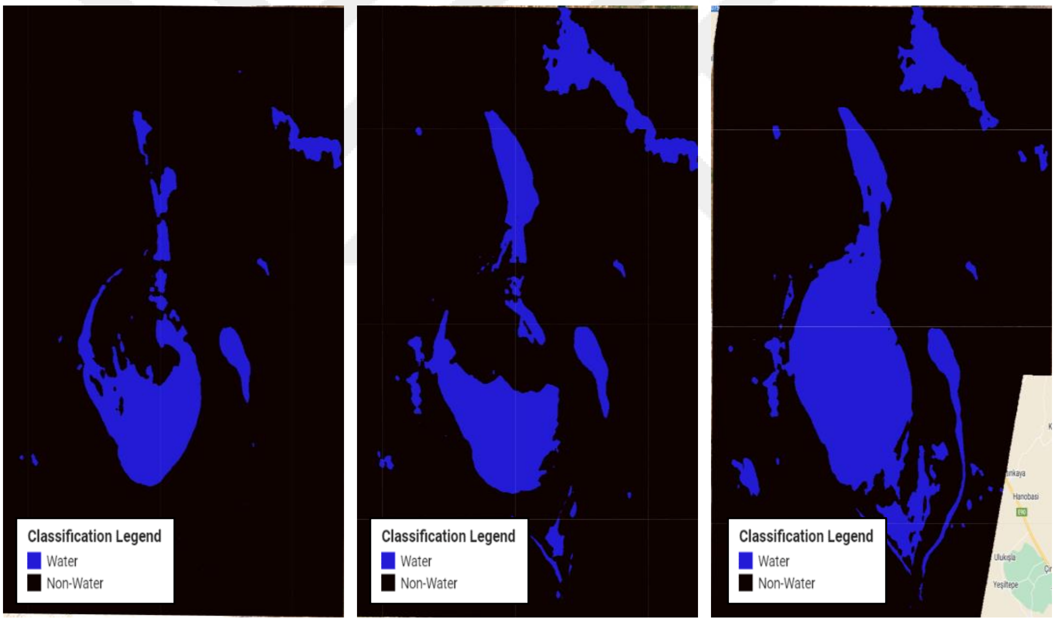

Figure 4.20. Classified Sentinel-2 images from 01/01/2023-12/01/2023 (a) to 18/06/2023-29/06/2023 (b) to 03/12/2023-15/12/2023 (c) in order

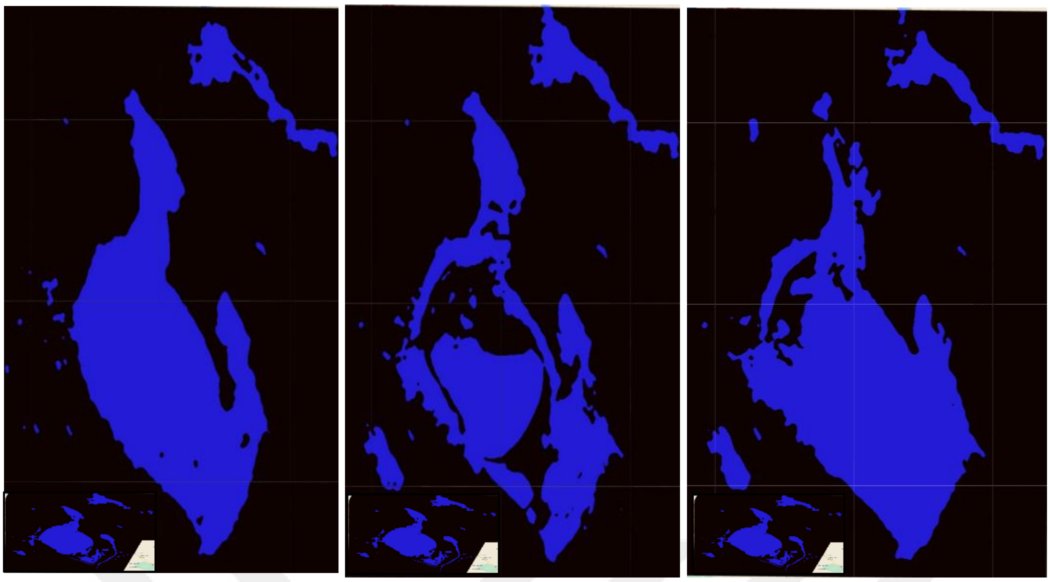

Figure 4.21. Classified Sentinel-1 images from 01/01/2023-12/01/2023 (a) to 18/06/2023-29/06/2023 (b) to 03/12/2023-15/12/2023 (c) in order

By visually comparing both these Sentinel-1 and Sentinel-2 classified images, we can see some obvious differences. In the January images we can see that Sentinel-1 classifies the whole lake area as water, while the Sentinel-2 image seems to misclassify a portion of the central- northern area of the lake as mostly non-water. Furthermore, much of the most northern area of the lake is misclassified as non-water. Even parts of Kizilirmak River in the north of Lake Tuz is shown to be misclassified as non-water by a large extent. In contrast, the June images seem to portray more similarities between each other regarding water coverage, Kizilirmak River is more prominent and both images show land left over in the central area of the lake due to water evaporation. Given the fact that this image was taken from June data, it stands to reason that parts of the lake would dry up as the summer heat increases. This similarity in water coverage is representative of the higher OA and PA (water) of the Sentinel-2 data compared to that of the January image. The December images however show yet again some differences in the water classification with much of the central-western region of the lake classified as non-water in the Sentinel-1 results, indicating shallower water levels or dry land. This is in contrast to the Sentinel-2 results which show that area being fully classified as water. The Sentinel-1 data does show a bit of misclassification of Kizilirmak River but this is most likely due to to wind increasing the radar backscatter from the water surfaces.

One of the primary reasons for Lake Tuz shrinking during the summer could be due to the high evaporation rate prevalent in the region during that season. The lake, being shallow with a depth of roughly 1-2 metres, is particularly susceptible to water loss through evaporation, especially when temperatures rise in the summer. The combination of high temperatures, low humidity, and prolonged sunlight intensifies the evaporation process, leading to a significant reduction in the lake's water volume and extent. Furthermore, the closed-basin nature of Lake Tuz contributes to its vulnerability to shrinking. As a closed basin, the lake has no outflow, meaning that water can only leave through evaporation. This lack of outflow further exacerbates the impact of high evaporation rates during the summer, as there is no replenishing water source to compensate for the water loss. Human activities, such as water extraction for salt production and agriculture, can also play a role in the lake's diminishment.

It should also be highlighted that most of the area of moist soil in the southern area of the lake was shown to have frequently high levels of classified water throughout the year. By visual inspection it can be seen that while there were some small water classifications in this area using Sentinel-2, the optical data did not show water cover to the same extent as Sentinel-1. This points to Sentinel-1 SAR data being extremely sensitive to moisture detection as it is very effective at detecting moisture in the soil surrounding the lake. This could be due to the inclusion of VH polarisation in the Sentinel-1 image due to the fact that VH polarisation has shown a stronger sensitivity to soil moisture changes compared to VV polarisation (Bousbih et al. 2017). In addition, using both VV and VH polarisations together has shown to improve soil moisture retrieval accuracy. This combination helps account for variations in vegetation and surface roughness, providing better correlation and reduced error margins in soil moisture estimates (Ma et al., 2020). Furthermore, seasonal flooding is known to take place in this area as stated in chapter 4.1.3, which would have increased water content in this area. It is to be emphasised that parts of this area were continuously marked as non-water by validation GCPs in both data sets throughout many parts of the year. This signifies that in the case of the southern portion of Lake Tuz, Sentinel-2 shows better results for water detection than Sentinel-1.

The classification accuracies of Lake Tuz from Sentinel-1 and Sentinel-2 data throughout 2023 reveal distinct differences in performance. Sentinel-1 consistently maintains a relatively high OA compared to that of Sentinel-2 data, predominantly around 0.85, with slight dips in March and September and peaks above 0.9 in December. The PA for water remains stable around 0.9, showing increased accuracy over the OA results. Both OA and PA show relatively stable trends with slight fluctuations, indicating more reliable performance of the Sentinel-1 data in water classification over Lake Tuz. Lower accuracies in specific periods, such as mid-April and late July, are minimal and do not significantly suggest overall bad performance but could be related to the drying of the lake in the summer months. As the water levels decreased, choosing validation GCPs became more of a challenge as the data used to choose validation points were not always completely clear as to where the water had dried up. Aside from that, the high consistency demonstrates that classification accuracy is less influenced by seasonal changes, atmospheric conditions, or sensor performance, compared to the Sentinel-2 data. Figure 4.22 shows the OA and PA (water) of the Sentinel-1 data throughout 2023.

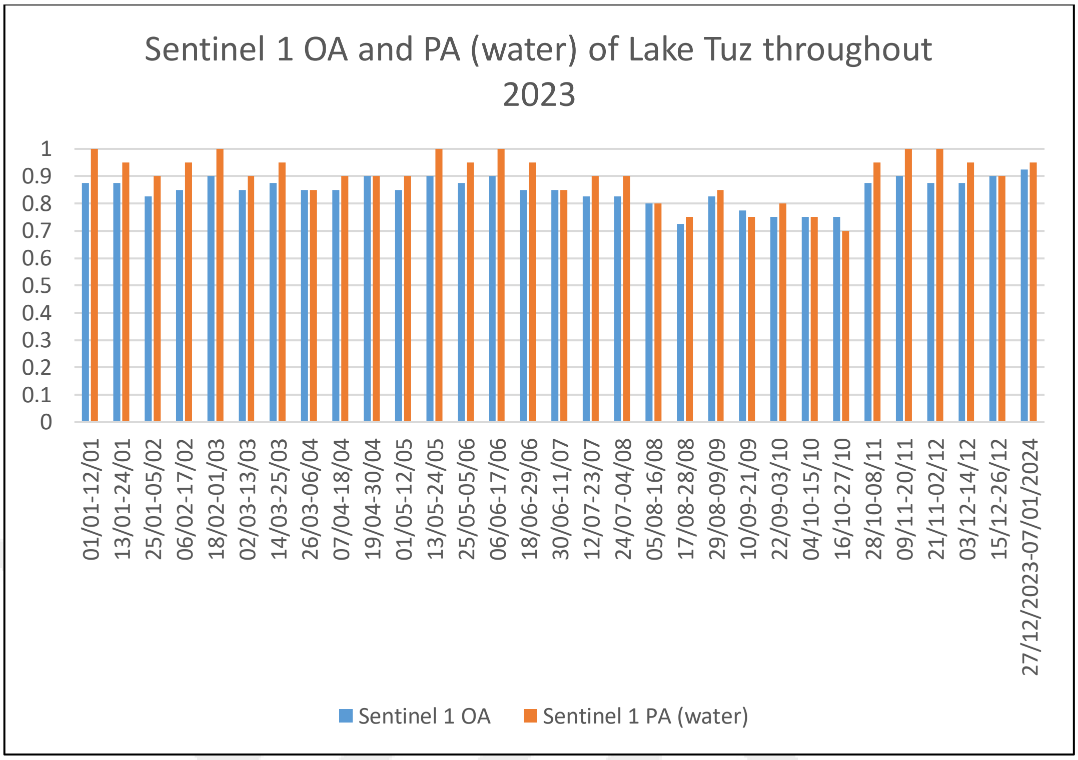

Figure 4.22. Table Showing OA and PA (water) of Sentinel-1 data on Lake Tuz throughout 2023

In contrast, Sentinel-2 shows lower and more variable OA, ranging from approximately 0.3 to 0.7, with peaks in mid-year and significant drops in March and late November. The PA for water also fluctuates considerably, ranging from near 0.1 to 0.8, with notable highs in July-August and lows in March and November. This comparison demonstrates Sentinel-1's increased reliability and consistency in classification accuracy, particularly for water, making it more effective for monitoring Lake Tuz. Sentinel-2, affected more by atmospheric conditions due to its optical nature, demonstrates higher variability and lower accuracy. Thus, Sentinel-1's radar data proves more advantageous for maintaining high classification accuracy throughout the year. Notably, the PA of water is generally higher than the OA throughout the year. This indicates that while the classifier is effective at identifying water pixels (producer's accuracy), the overall classification performance across all classes is slightly lower. This disparity suggests that while water is being detected with reasonable accuracy, the inclusion of other classes in the overall accuracy calculation lowers the average. More classes ultimately add to the complexity of the classification process and thus can lead to more inaccuracies. This ultimately led to a situation where parts of the lake that should be classified as water were fairly regularly classified as something else. Sentinel-1 PA for water is still however shown to be higher than that of Sentinel-2, and given that water detection is the primary goal of this study, Sentinel-2 failed to keep up with Sentinel-1 in this regard. Figure 4.23 shows the OA and PA (water) of the Sentinel-2 data throughout 2023.

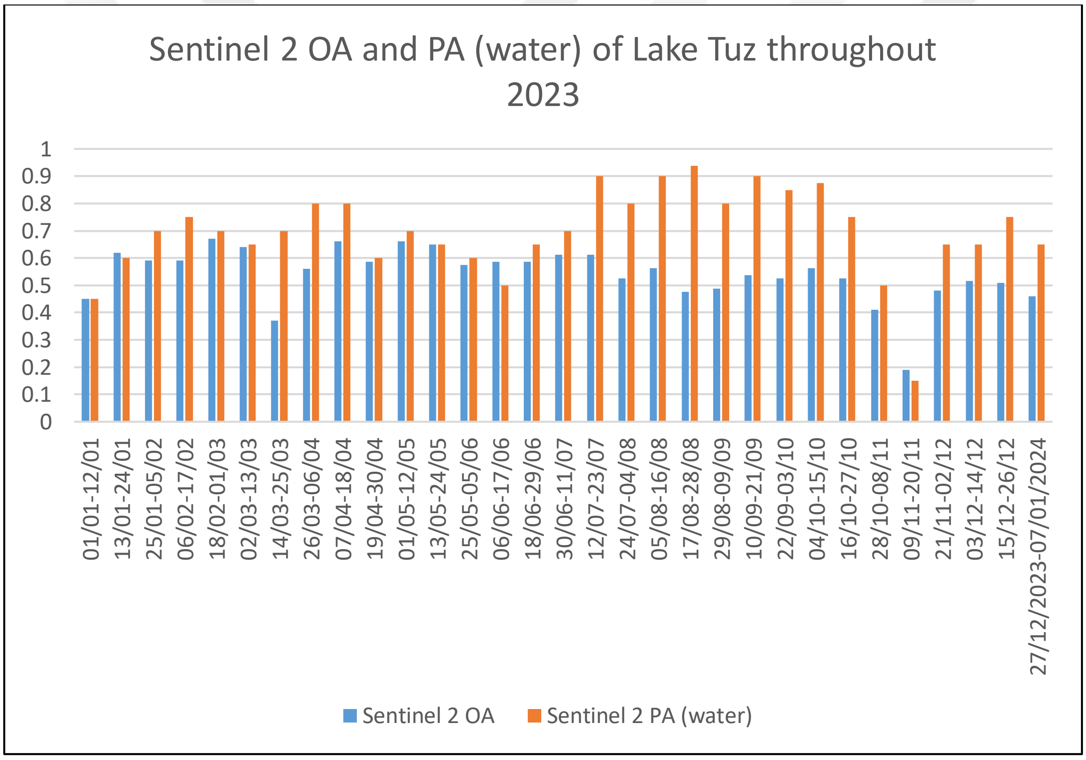

Figure 4.23. Table Showing OA and PA (water) of Sentinel-2 data on Lake Tuz throughout 2023

Overall, the highest Sentinel-2 accuracies for both OA and PA occur mostly during the spring and late summer periods, indicating potentially more stable weather conditions or better sensor performance during these times. Lower accuracies in certain periods, such as early March and late November, could be due to seasonal changes, increased cloud cover, or other environmental factors affecting classification accuracy.

4.4 Results and Discussion Summary

The results from this study provide an analysis of the accuracy and effectiveness of Sentinel-1 and Sentinel-2 imagery in classifying water bodies across multiple lakes. The findings demonstrate that the use of cumulative training data from various regions can significantly affect the overall accuracy depending on the data used. Sentinel-1 consistently showed higher reliability and accuracy, particularly in detecting water bodies with varying textures and moisture levels, as evidenced by its superior OA and PA values. Conversely, Sentinel-2, although effective, faced challenges due to cloud cover and the spectral complexities of water, vegetation, and other classes. The only situation where Sentinel-2 showed better results was when classifying the southern portion of Lake Tuz, where Sentinel-1 classified the smooth surface of moist soil as water, Sentinel-2 did not.

When training the RFC on only Lake Tuz for the purposes of classifying Lake Tuz, Sentinel-1 data was shown to have a relatively negligible difference in accuracies when compared to the accuracy of classifying Lake Tuz using an RFC trained on lakes globally. On the other hand, Sentinel-2 data showed a much higher accuracy when classifying Lake Tuz using the RFC trained only on Lake Tuz, suggesting that training an RFC on multiple global ROIs to classify Lake Tuz has a detrimental effect when classifying Sentinel-2 images. This is in contrast to classifying Sentinel-1 images, which does not show a huge difference in accuracies.

Sentinel-1's sensitivity to moisture and surface roughness, while beneficial for detecting water bodies in diverse conditions, can lead to overestimations in areas with moist soil or smooth salt crusts. The inclusion of VH polarisation in conjunction with VV polarisation in the Sentinel-1 data could have further contributed to this sensitivity. Furthermore, VH polarisation is known to be more responsive to soil moisture variations but when training the classifier, was found to have a lower importance value of 22.11 compared to the higher importance value of 31.82 for the VV polarisation. This higher importance of VV influencing classification indicates that areas of moist soil and salt crust areas were very smooth given that they were classified as water. This is due to the fact that VV polarisation tends to be much more sensitive to surface roughness than VH, especially in the C-band used by Sentinel-1, leading to potential misclassification. (Kweon and Oh, 2013).

To expand on this, the presence of seasonal flooding in this area likely exacerbated this effect, leading to even higher water detections by Sentinel-1. In contrast, Sentinel-2's optical data, while less sensitive to moisture and surface roughness, faced challenges in accurately classifying water bodies due to cloud cover and the spectral complexities of the lake's environment. The presence of salt deposits, shallow water depths, and algal blooms can alter the spectral signature of the water, making it difficult for optical sensors to distinguish between water and other land cover types. This was evident in the misclassification of water as non-water classes in certain regions of Lake Tuz, particularly during periods of high cloud cover or in areas with mixed land cover types. The lower overall accuracy and producer's accuracy for water in Sentinel-2 data throughout the year further emphasises these challenges. The comparative analysis highlights Sentinel-1's efficiency at detecting water even in diverse environmental conditions, making it more suitable for continuous water body monitoring. One exception however of Sentinel-2 data showing a general low PA for water is demonstrated within the late summer and early autumn months, where Sentinel-2's PA is shown to be generally higher than that of Sentinel-1's PA. This indicates that during this period where the lake seemed to shrink the most, Sentinel-2 was more effective at accurately detecting water, with Sentinel-1 again being too sensitive to the smooth surfaces of salt crust.

CHAPTER 5

CONCLUSION

5.1 Discussion

This research has successfully demonstrated the use of Synthetic Aperture Radar (SAR) and optical remote sensing technologies to monitor and analyse the water extents of various lakes, with a primary focus on Lake Tuz in Turkiye. The study revealed several key points. Firstly, the study employed the Random Forest Classifier (RFC) to classify land cover types and detect water extents. The results indicated that training a classifier on multiple world-wide ROIs with machine learning techniques maintains consistently high classification accuracy and water monitoring capabilities for Sentinel-1 data. In contrast, the same technique did not prove as effective when applied to the Sentinel-2 data, with evidence showing that higher accuracy could be obtained from training only on the ROI being classified, Lake Tuz. The same cannot be said for classifying Sentinel-1 data, which shows that training on other ROIs globally did not decrease accuracy in any significant way, but did not improve accuracy either. Ultimately the advantages of SAR over optical data were apparent, as SAR data from Sentinel-1, proved effective in detecting water bodies despite atmospheric conditions like cloud cover. It provided reliable data for analysing water extents in comparison to optical data from Sentinel-2. Secondly, the extent of water levels diminishing on Lake Tuz are evident, with significant water volume declines due to factors including climate change, increased temperatures, evaporation rates, and anthropogenic activities. The findings showed that Lake Tuz's water extent fluctuates significantly throughout the year, influenced by seasonal factors, climate change, and human activities such as excessive water withdrawal.

The research demonstrates the importance of remote sensing technologies and machine learning algorithms in environmental monitoring. The ability to accurately classify and monitor water bodies has significant implications for understanding climate change impacts, managing water resources, and developing effective conservation strategies. The integration of SAR and optical data offers a robust approach to overcoming the limitations of each technology when used independently.

5.2 Limitations and Future Recommendations

Despite the study's results, several limitations were identified. Data limitations included high cloud cover impacting the accuracy of optical data classification. The geographical scope, while including multiple lakes globally, primarily focused on Lake Tuz, suggesting broader studies could include more diverse geographical areas for comprehensive insights. Additionally, while effective, the Random Forest Classifier may not be the best fit for all types of land cover classification, indicating that exploring other machine learning algorithms could provide different perspectives and potentially higher accuracies.

Ultimately, many of Lake Tuz’s water areas were classified incorrectly using the Sentinel-2 data, instead being classified as non-water classes such as urban, occasionally snow and frequently vegetation. This led to a generally smaller calculated water extent as water was classified incorrectly. On the other hand, Sentinel-1 data misclassified one specific area of non-water as water due to SAR’s sensitivity to moisture and smooth surfaces, leading to a larger calculated water extent. Based on this data, Sentinel-2 data appears to be better at not making such mistakes with moist soil and smooth salt crust but in contrast, Sentinel-1 does not make mistakes regarding misclassification of water due to cloud cover or other factors. Despite this, much of Sentinel-2’s lower overall accuracy was due to the inclusion of other non-water classes, adding complexity to the RFC when trained on multiple other ROIs. However, with the exception of a generally higher PA of water during the late summer and early autumn months, the lower producer’s accuracy of water across the year shows that in many instances water was being classified as something else, leading to a smaller calculated water extent of the ROI. This is the opposite case of the Sentinel-1 data. It can be surmised from this that the real water coverage of the ROI of Lake Tuz lies somewhere between that of the calculated Sentinel-1 data and Sentinel-2 data.

To build on the findings of this study, future research could focus on several areas. Conducting more extended multi-temporal studies could analyse long-term trends in water extents and their correlations with climate variables. Utilising additional remote sensing data sources, such as ground-based observations, could enhance the accuracy and reliability of classifications. Exploring and comparing other deep learning and machine learning algorithms, such as Convolutional Neural Networks (CNN) and Support Vector Machines (SVM), could determine the most effective methods for land cover classification. Expanding the study to include more lakes and diverse regions would help generalise the findings and understand global patterns in water body changes. Moreover, fusing both Sentinel-1 and Sentinel-2 images for training and classification could also provide more accurate results for water detection, ideally obtaining the best of both worlds so as to not end up with erroneously increased or decreased calculated water coverage.

Based on the findings, several practical recommendations are proposed. Authorities should use remote sensing data to monitor and manage water resources effectively, ensuring sustainable water use and mitigating the impacts of climate change. Developing targeted conservation strategies to protect shrinking water bodies, focusing on mitigating human impacts and adapting to climate changes, is crucial. Policymakers should incorporate remote sensing data in environmental regulations and water management policies to ensure data-driven decision-making.

To conclude, this research demonstrates the importance of integrating advanced technologies in environmental monitoring. The use of SAR and optical remote sensing, combined with machine learning techniques, offers a powerful tool for understanding and managing the impacts of climate change on vital water resources. The benefits and limitations of training a classifier on multiple different environments are brought forward. Additionally, insight onto the annual dynamics of Lake Tuz in Turkiye is brought under intense scrutiny, a lake that has been heavily affected by climate change over the past decades. Future studies and continued advancements in technology will further enhance our capabilities, contributing to the sustainability and conservation of our planet's ecosystems. This thesis journey demonstrates the significance of interdisciplinary approaches in tackling complex environmental challenges, paving the way for more informed and effective solutions.

REFERENCES

Abarca-Del-Rio, R., Crétaux, J.F., Berge-Nguyen, M. and Maisongrande, P., 2012. Does Lake Titicaca still control the Lake Poopó system water levels? An investigation using satellite altimetry and MODIS data (2000–2009). Remote sensing letters, 3(8), pp.707-714.

Abdikan, S., Sanli, F.B., Ustuner, M. and Calò, F., 2016. Land cover mapping using sentinel-1 SAR data. *The International Archives of the Photogrammetry, Remote Sensing and Spatial Information Sciences*, *41*, pp.757-761.

Akar, Ö. and Güngör, O., 2015. Integrating multiple texture methods and NDVI to the Random Forest classification algorithm to detect tea and hazelnut plantation areas in northeast Turkey. *International Journal of Remote Sensing*, *36*(2), pp.442-464.

Aydin-Kandemir, F. and Erlat, E., 2023. Assessment of the relationship of the salt-covered area and the groundwater storage/drought indicators in the disappearing Lake Tuz in Turkey (1985–2021). *Environmental Monitoring and Assessment*, *195*(2), p.333.

Bayik, C., Abdikan, S., Ozbulak, G., Alasag, T., Aydemir, S., & Balik Sanli, F. (2018). Exploiting multi- temporal sentinel-1 SAR data for flood extent mapping. The International Archives of the Photogrammetry, Remote Sensing and Spatial Information Sciences, XLII-3/W4, 109–113. https://doi.org/10.5194/isprs- archives xlii-3-w4-109-2018

Bilgilioğlu, B.B., Erten, E. and Musaoğlu, N., 2021. Analysis of Salt Lake Volume dynamics using Sentinel-1 based SBAS measurements: A case study of Lake Tuz, Turkey. *Remote Sensing*, *13*(14), p.2701.

Bousbih, S., Zribi, M., Lili-Chabaane, Z., Baghdadi, N., El Hajj, M., Gao, Q. and Mougenot, B., 2017. Potential of Sentinel-1 radar data for the assessment of soil and cereal cover parameters. Sensors, 17(11), p.2617.

Bozdag, A. FatihTemiz, A.B., Durduran, S.S. and Gumus, M.G., 2017. Monitoring coastline change using remote sensing and gis technology: a case study of Burdur Lake, Turkey. *FEB-FRESENIUS ENVIRONMENTAL BULLETIN*, p.7235.

Breiman, L., 2001. Random forests. *Machine learning*, *45*, pp.5-32.

Brown, C.F., Brumby, S.P., Guzder-Williams, B., Birch, T., Hyde, S.B., Mazzariello, J., Czerwinski, W., Pasquarella, V.J., Haertel, R., Ilyushchenko, S. and Schwehr, K., 2022. Dynamic World, Near real-time global 10 m land use land cover mapping. *Scientific Data*, *9*(1), p.251.

Chan, Y.K. and Koo, V., 2008. An introduction to synthetic aperture radar (SAR). *Progress In Electromagnetics Research B*, *2*, pp.27-60.

Clement, M.A., Kilsby, C.G. and Moore, P., 2018. Multi-temporal synthetic aperture radar flood mapping using change detection. *Journal of Flood Risk Management*, *11*(2), pp.152-168.

Dengiz, O., Ozcan, H., Koksal, E.S., Baskan, O. and Kosker, Y., 2010. Sustainable natural resource management and environmental assessment in the Salt Lake (Tuz Golu) Specially Protected Area. *Environmental monitoring and assessment*, *161*, pp.327-342.

Dervisoglu, A., Yağmur, N., Fıratlı, E., Musaoğlu, N. and Tanık, A., 2022. Spatio-temporal assessment of the shrinking Lake Burdur, Turkey. *International Journal of Environment and Geoinformatics*, *9*(2), pp.169-176.

Drusch, M., Del Bello, U., Carlier, S., Colin, O., Fernandez, V., Gascon, F., Hoersch, B., Isola, C., Laberinti, P., Martimort, P. and Meygret, A., 2012. Sentinel-2: ESA's optical high-resolution mission for GMES operational services. *Remote sensing of Environment*, *120*, pp.25-36.

Elwan, E., Le Page, M., Jarlan, L., Baghdadi, N., Brocca, L., Modanesi, S., Dari, J., Quintana Seguí, P. and Zribi, M., 2022. Irrigation mapping on two contrasted climatic contexts using Sentinel-1 and Sentinel-2 data. *Water*, *14*(5), p.804.

Fernández, D.G., López, R.S., Briceño, N.B.R., López, J.O.S. and Oliva, M., 2022. Dynamics of the Burlan and Pomacochas Lakes Using SAR Data in GEE, Machine Learning Classifiers, and Regression Methods. *ISPRS International Journal of Geo-Information*, *11*(11), p.534.

Ferrara, M., Jackson, J.A. and Austin, C., 2009, April. Enhancement of multi-pass 3D circular SAR images using sparse reconstruction techniques. In *Algorithms for Synthetic Aperture Radar Imagery XVI* (Vol. 7337, pp. 9-18). SPIE.

Firatli, E., Dervisoglu, A., Yagmur, N., Musaoglu, N. and Tanik, A., 2022. Spatio-temporal assessment of natural lakes in Turkey. *Earth Science Informatics*, *15*(2), pp.951-964.

Flores-Anderson, A.I., Herndon, K.E., Thapa, R.B. and Cherrington, E., 2019. *The SAR handbook: comprehensive methodologies for forest monitoring and biomass estimation* (No. MSFC-E-DAA-TN67454).

Forsyth, B. and Güzel, S., 2024. A Comparison of Image Classification on Synthetic Aperture Radar and Optical Images for Detection of Water Bodies Case of Lake Burdur, Türkiye. *International Journal of Water Management and Diplomacy*, *1*(7), pp.47-61.

Fu, J., Wang, J. and Li, J., 2008, February. Study on the automatic extraction of water body from TM image using decision tree algorithm. In *International*

Symposium on Photoelectronic Detection and Imaging 2007: Related Technologies and Applications (Vol. 6625, pp. 17-25). SPIE.

Ge, P., Gokon, H., and Meguro, K. (2019). Building Damage Assessment Using Intensity SAR Data with Different Incidence Angles and Longtime Interval. Journal of Disaster Research, 14(3), 456-465. doi:10.20965/jdr.2019.p0456

Gislason, P.O., Benediktsson, J.A. and Sveinsson, J.R., 2006. Random forests for land cover classification. *Pattern recognition letters*, *27*(4), pp.294-300.

Google (2024) *Sentinel 1 algorithms.* Available at: https://developers.google.com/earth-engine/guides/sentinel1 (Accessed: 16 April 2024)

Guo, M., Li, J., Sheng, C., Xu, J. and Wu, L., 2017. A review of wetland remote sensing. *Sensors*, *17*(4), p.777.

Hannoun, D. and Tietjen, T., 2023. Lake management under severe drought: lake mead, Nevada/Arizona. *JAWRA Journal of the American Water Resources Association*, *59*(2), pp.416-428.

Hassanzadeh, E., Zarghami, M. and Hassanzadeh, Y., 2012. Determining the main factors in declining the Urmia Lake level by using system dynamics modeling. *Water Resources Management*, *26*, pp.129-145.

Hastie, T., Tibshirani, R., Friedman, J.H. and Friedman, J.H., 2009. *The elements of statistical learning: data mining, inference, and prediction* (Vol. 2, pp. 1-758). New York: springer.

Hua, A.K., 2017. Land use land cover changes in detection of water quality: a study based on remote sensing and multivariate statistics. *Journal of environmental and public health*, *2017*.

Huang, C., Chen, Y., Zhang, S. and Wu, J., 2018. Detecting, extracting, and monitoring surface water from space using optical sensors: A review. *Reviews of Geophysics*, *56*(2), pp.333-360.

Huang, W., DeVries, B., Huang, C., Lang, M.W., Jones, J.W., Creed, I.F. and Carroll, M.L., 2018. Automated extraction of surface water extent from Sentinel-1 data. *Remote Sensing*, *10*(5), p.797.

Iban, M.C. and Sekertekin, A., 2022. Machine learning based wildfire susceptibility mapping using remotely sensed fire data and GIS: A case study of Adana and Mersin provinces, Turkey. *Ecological Informatics*, *69*, p.101647.

Keith, D.J., 2020. Algal Bloom Monitoring: Remote Sensing. In *Fresh Water and Watersheds* (pp. 265-276). CRC Press.

Krieger, G., Hajnsek, I., Papathanassiou, K.P., Younis, M. and Moreira, A., 2010. Interferometric synthetic aperture radar (SAR) missions employing formation flying. *Proceedings of the IEEE*, *98*(5), pp.816-843.

Kweon, S.K. and Oh, Y., 2013. Estimation of soil moisture and surface roughness from single-polarized radar data for bare soil surface and comparison with dual-and quad-polarization cases. IEEE Transactions on Geoscience and Remote Sensing, 52(7), pp.4056-4064.

Lary, D.J., Alavi, A.H., Gandomi, A.H. and Walker, A.L., 2016. Machine learning in geosciences and remote sensing. Geoscience Frontiers, 7(1), pp.3-10.

Lima-Quispe, N., Escobar, M., Wickel, A.J., von Kaenel, M. and Purkey, D., 2021. Untangling the effects of climate variability and irrigation management on water levels in Lakes Titicaca and Poopó. *Journal of Hydrology: Regional Studies*, *37*, p.100927.

Manandhar, R., Odeh, I.O. and Ancev, T., 2009. Improving the accuracy of land use and land cover classification of Landsat data using post-classification enhancement. *Remote Sensing*, *1*(3), pp.330-344.

Moreira, A., Prats-Iraola, P., Younis, M., Krieger, G., Hajnsek, I. and Papathanassiou, K.P., 2013. A tutorial on synthetic aperture radar. *IEEE Geoscience and remote sensing magazine*, *1*(1), pp.6-43.

Peker, E.A., 2019. *Spatio-temporal changes of lake water extents in lakes region (Turkey) using remote sensing* (Master's thesis, Middle East Technical University).

Quan, Y., Tong, Y., Feng, W., Dauphin, G., Huang, W. and Xing, M., 2020. A novel image fusion method of multi-spectral and sar images for land cover classification. *Remote Sensing*, *12*(22), p.3801.

Rokni, K., Ahmad, A., Selamat, A. and Hazini, S., 2014. Water feature extraction and change detection using multitemporal Landsat imagery. *Remote sensing*, *6*(5), pp.4173-4189.

Sola, I., García-Martín, A., Sandonís-Pozo, L., Álvarez-Mozos, J., Pérez-Cabello, F., González-Audícana, M. and Llovería, R.M., 2018. Assessment of atmospheric correction methods for Sentinel-2 images in Mediterranean landscapes. *International journal of applied earth observation and geoinformation*, *73*, pp.63-76.

Souza, W.D.O., Reis, L.G.D.M., Ruiz-Armenteros, A.M., Veleda, D., Ribeiro Neto, A., Fragoso Jr, C.R., Cabral, J.J.D.S.P. and Montenegro, S.M.G.L., 2022. Analysis of environmental and atmospheric influences in the use of SAR and optical imagery from Sentinel-1, Landsat-8, and Sentinel-2 in the operational monitoring of reservoir water level. *Remote Sensing*, *14*(9), p.2218.

Twele, A., Cao, W., Plank, S. and Martinis, S., 2016. Sentinel-1-based flood mapping: a fully automated processing chain. *International Journal of Remote Sensing*, *37*(13), pp.2990-3004.

Ulaby, F.T., 1981. *Microwave remote sensing. vol. 2*.

Wang, M., Mao, D., Xiao, X., Song, K., Jia, M., Ren, C. and Wang, Z., 2023. Interannual changes of coastal aquaculture ponds in China at 10-m spatial resolution during 2016–2021. Remote Sensing of Environment, 284, p.113347.

Wang, Y., Ruan, R., She, Y. and Yan, M., 2011. Extraction of water information based on RADARSAT SAR and Landsat ETM+. *Procedia Environmental Sciences*, *10*, pp.2301-2306.

Wangchuk, S. and Bolch, T., 2020. Mapping of glacial lakes using Sentinel-1 and Sentinel-2 data and a random forest classifier: Strengths and challenges. *Science of Remote Sensing*, *2*, p.100008.

Wu, S., Fan, P., Fan, W. and Wu, Y., 2023. Research on Water Level Changes in Lake Mead. *Highlights in Science, Engineering and Technology*, *31*, pp.7-12.

Yagmur, N., Bilgilioglu, B.B., Dervisoglu, A., Musaoglu, N. and Tanik, A., 2021. Long and short-term assessment of surface area changes in saline and freshwater lakes via remote sensing. *Water and Environment Journal*, *35*(1), pp.107-122.

Ceyhan, E., 2016. Multi-temporal water extent analysis of a hypersaline playa lake using landsat imagery (Master's thesis, Middle East Technical University).

APPENDICES

A. Classified Sentinel-1 images of Lake Tuz

In this section are all the classified images of Lake Tuz in order from January to December throughout 2023 that were not present in the main body of the thesis.

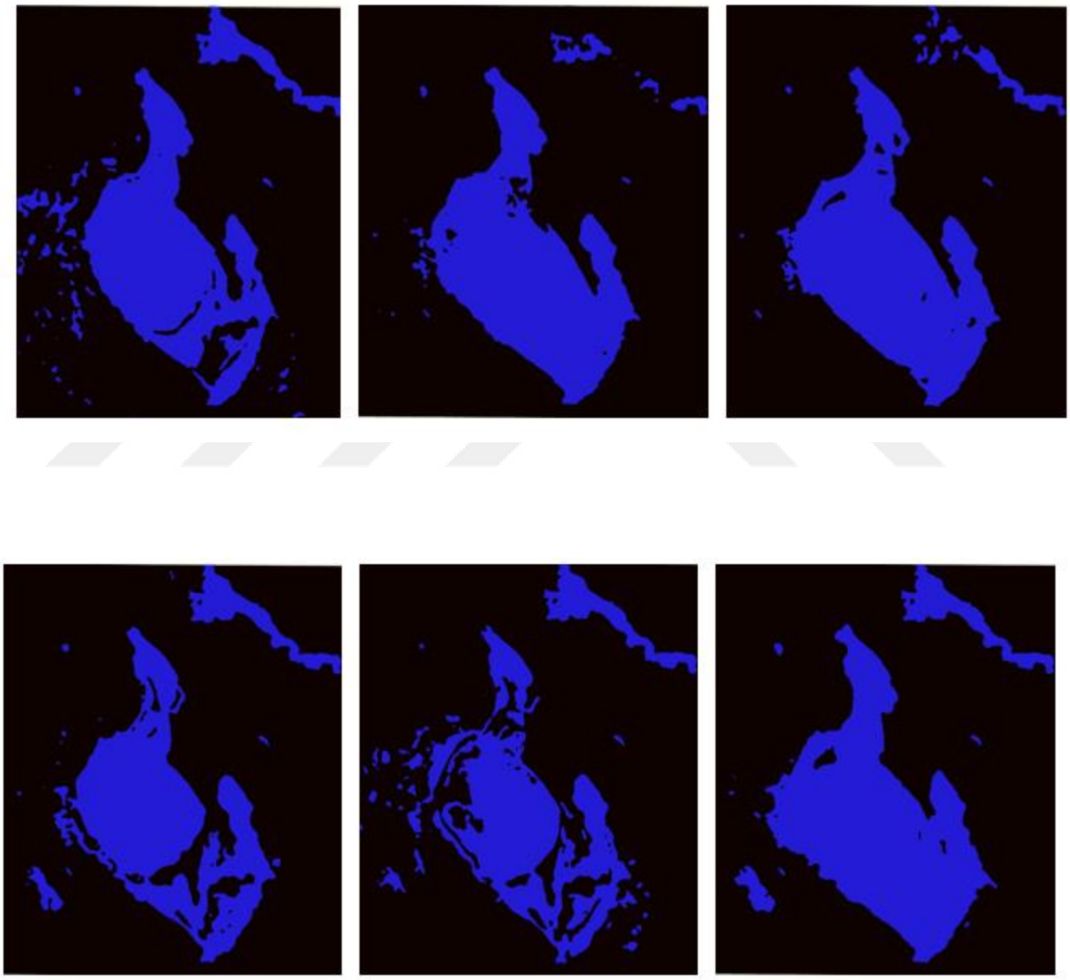

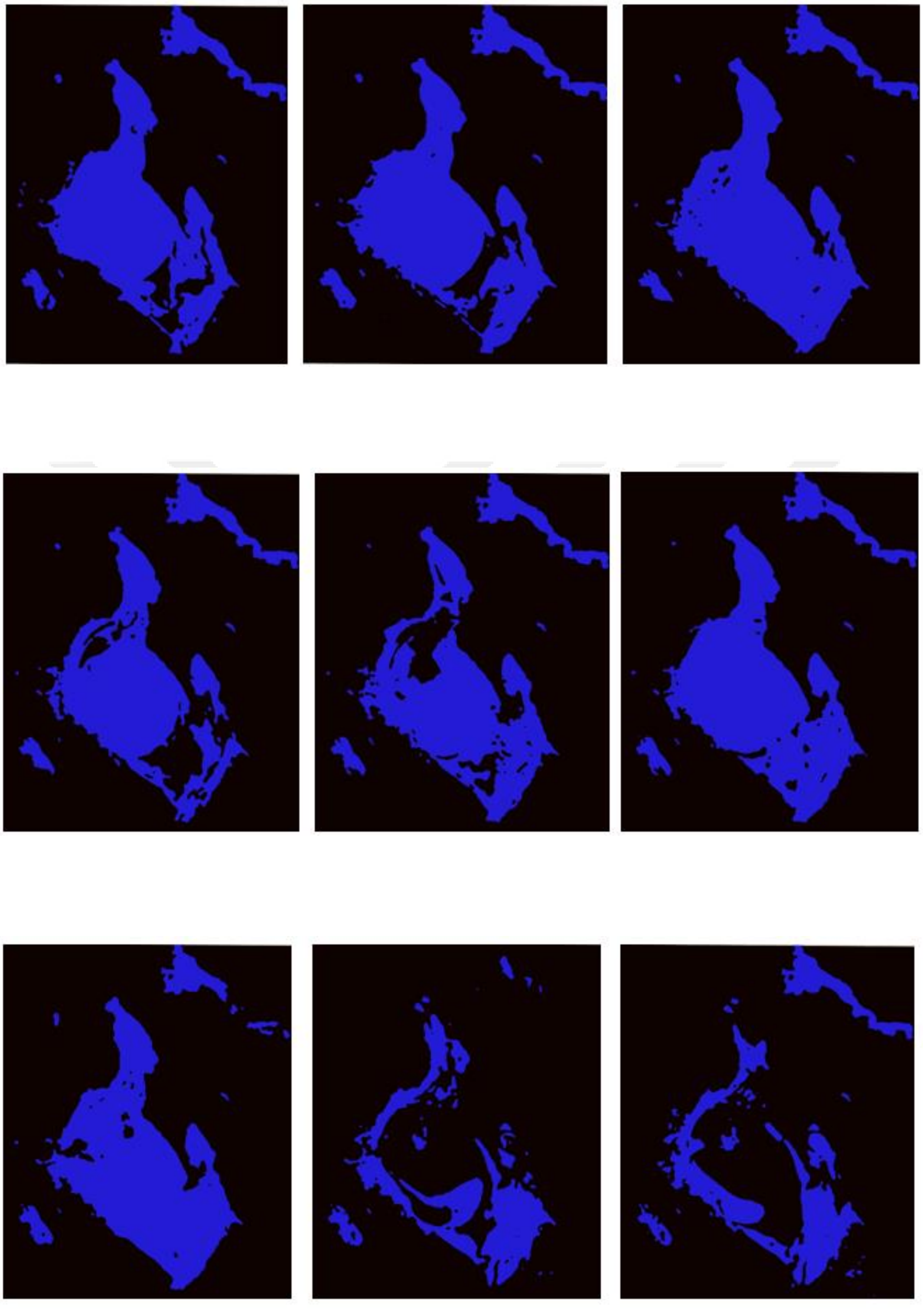

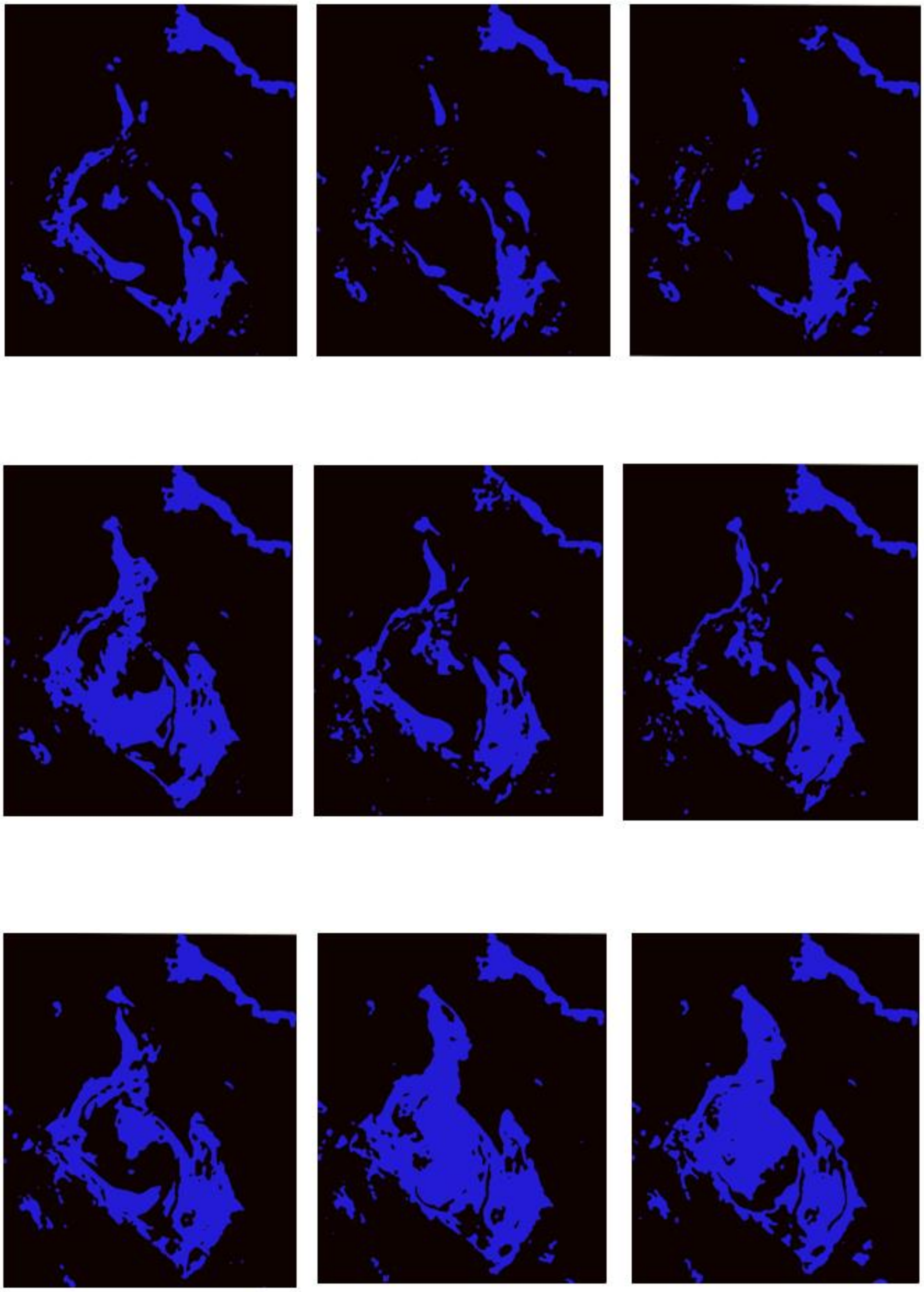





B. Classified Sentinel-2 images of Lake Tuz

In this section are all the classified images of Lake Tuz in order from January to December throughout 2023 that were not present in the main body of the thesis.